University of Kent

Kent Academic Repository

Del Rosario, Joanne Marie M., Vishwanath, Sneha, Frost, Simon D.W., Sujit, Sneha B., Ashokan, Sruthika K., Vendramelli, Robert, Ferrari, Matteo, Carnell, George W., Vianello, Lucrezia, Pagliari, Matteo and others (2026) *Broad vaccine protection against globally diverse influenza A/H5Nx viruses.* Cell Reports Medicine . ISSN 2666-3791.

Downloaded from

https://kar.kent.ac.uk/117574/ The University of Kent's Academic Repository KAR

The version of record is available from

https://doi.org/10.1016/j.xcrm.2026.103131

This document version

Publisher pdf

DOI for this version

Licence for this version

CC BY (Attribution)

Additional information

Versions of research works

Versions of Record

If this version is the version of record, it is the same as the published version available on the publisher's web site. Cite as the published version.

Author Accepted Manuscripts

If this document is identified as the Author Accepted Manuscript it is the version after peer review but before type setting, copy editing or publisher branding. Cite as Surname, Initial. (Year) 'Title of article'. To be published in ***Title of Journal*** , Volume and issue numbers [peer-reviewed accepted version]. Available at: DOI or URL (Accessed: date).

Enquiries

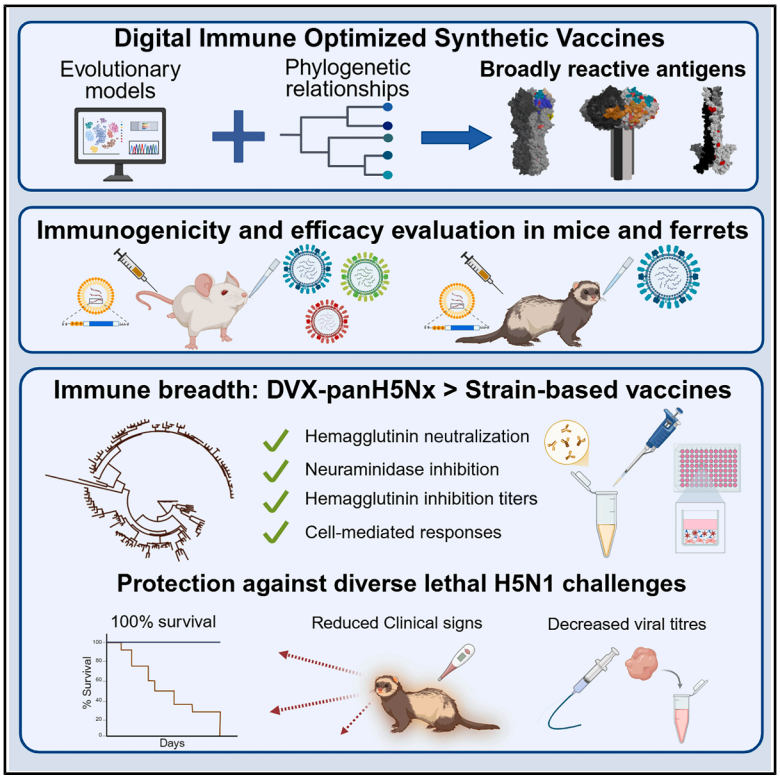
If you have questions about this document contact ResearchSupport@kent.ac.uk. Please include the URL of the record in KAR. If you believe that your, or a third party's rights have been compromised through this document please see our Take Down policy (available from https://www.kent.ac.uk/guides/kar-the-kent-academic-repository#policies).

Cell Reports
Medicine

Article

Broad vaccine protection against globally diverse influenza A/H5Nx viruses

Graphical abstract



Authors

Joanne Marie M. Del Rosario, Sneha Vishwanath, Simon D.W. Frost, ..., Darwyn Kobasa, Francesco Bonfante, Jonathan L. Heeney

Correspondence

jlh66@cam.ac.uk

In brief

Del Rosario et al. employ digitally immune-optimized synthetic vaccine technology to engineer a multi-antigen mRNA vaccine that confers broad immunogenicity and protection against globally distinct and evolving H5Nx influenza viruses. This demonstrates that computationally designed multivalent antigens can be harnessed as preparedness tools against contemporary and future H5Nx diversity.

Highlights

- Computationally engineered HA, NA, and M2 antigens are combined as a panH5Nx vaccine
- Vaccine protection against lethal H5N1 clade 1, 2.3.2.1e, and 2.3.4.4b challenges
- Superior survival over strain-based candidate vaccine virus (CVV) vaccines
- Protection correlates with combined HA-neutralizing and NA-inhibiting immunity

Del Rosario et al., 2026, Cell Reports Medicine 7, 103131
November 17, 2026 Crown Copyright © 2026 Published by Elsevier Inc.
https://doi.org/10.1016/j.xcrm.2026.103131

CellPress

Please cite this article in press as: Del Rosario et al., Broad vaccine protection against globally diverse influenza A/H5Nx viruses, Cell Reports Medicine (2026), https://doi.org/10.1016/j.xcrm.2026.103131

Cell Reports Medicine

CellPress
OPEN ACCESS

Article

Broad vaccine protection against globally diverse influenza A/H5Nx viruses

Joanne Marie M. Del Rosario,[1] Sneha Vishwanath,[2] Simon D.W. Frost,[1,3,4] Sneha B. Sujit,[1] Sruthika K. Ashokan,[1] Robert Vendramelli,[5] Matteo Ferrari,[1] George W. Carnell,[6] Lucrezia Vianello,[7] Matteo Pagliari,[7,8] Sami Ramzi,[7,9] Valentina Maria Panzarin,[7] Elisa Mazzacan,[7] Andrea Fortin,[7] Marta Vascellari,[10] Thang Truong,[5] Paul Tonks,[2] Ana Liza Ortiz,[11] Chloe Qingzhou Huang,[2] Sebastian Einhauser,[12] Michael Schachtner,[12] Benedikt Asbach,[12] Daniel Matthew L. Storisteanu,[2] Nigel J. Temperton,[13] Matthew N. Davies,[1] David Moss,[1] Rebecca Kinsley,[1] Ralf Wagner,[1,12,14] Darwyn Kobasa,[5,15] Francesco Bonfante,[7] and Jonathan L. Heeney[1,2,16,*]

[1]DIOSynVax, West Cambridge Campus, Cambridge CB3 0ES, UK
[2]Lab of Viral Zoonotics, Department of Veterinary Medicine, University of Cambridge, Cambridge CB3 0ES, UK
[3]London School of Hygiene and Tropical Medicine, London WC1E 7HT, UK
[4]Microsoft Health Futures, Redmond, WA 98052, USA
[5]Special Pathogens Program, National Microbiology Laboratory, Public Health Agency of Canada, Winnipeg, MB R3E 3R2, Canada
[6]One Virology, Wolfson Centre for Global Virus Research, School of Veterinary Medicine and Science, University of Nottingham, Nottingham LE12 5RD, UK
[7]Division of Comparative Biomedical Sciences, Istituto Zooprofilattico Sperimentale delle Venezie (IZSVe), Legnaro, 35020 Padua, Italy
[8]Department for Women's and Children's Health, University of Padua, 35128 Padova, Italy
[9]Department of Animal Medicine, Production and Health, University of Padua, Legnaro, 35020 Padova, Italy
[10]Diagnostic Services Histopathology and Parasitology Department and Animal Experimentation and Welfare Division, Istituto Zooprofilattico Sperimentale delle Venezie (IZSVe), Legnaro, Padua 35020, Italy
[11]Department of Veterinary Medicine, University of Cambridge, Cambridge CB3 0ES, UK
[12]Institute of Medical Microbiology and Hygiene, University of Regensburg, 93053 Regensburg, Germany
[13]Viral Pseudotype Unit, Medway School of Pharmacy, The Universities of Greenwich and Kent at Medway, Chatham ME4 4TB, UK
[14]Institute of Clinical Microbiology & Hygiene, University Hospital, University of Regensburg, 93053 Regensburg, Germany
[15]Department of Medical Microbiology and Infectious Diseases, University of Manitoba, Winnipeg, MB R3E 0J9, Canada
[16]Lead contact
*Correspondence: jlh66@cam.ac.uk
https://doi.org/10.1016/j.xcrm.2026.103131

SUMMARY

Influenza A/H5Nx viruses continue to diversify and undergo gene reassortment as they infect avian and mammalian hosts worldwide. The severity of human infections varies substantially between different H5 clades and neuraminidase (NA) reassortants, creating unpredictable pandemic risk. Existing H5 vaccines, typically based on a single hemagglutinin (HA) strain, cannot keep pace with this natural variation. To address this problem, we computationally engineer HA, NA, and M2 antigens representing the global antigenic space of circulating H5Nx viruses, prioritizing N1 and N6 subtypes associated with the highest threat in humans. The resulting digitally immune-optimized mRNA vaccine, DVX-panH5Nx, elicits broad HA neutralization and NA inhibition across divergent clades in mice and ferrets. Compared to WHO candidate vaccine viruses (CVVs), DVX-panH5Nx confers superior protection against antigenically distinct H5N1 challenges spanning two decades of viral evolution, demonstrating that computationally designed multivalent antigen vaccines can overcome natural influenza diversification and provide a scalable strategy for pre-pandemic preparedness.

INTRODUCTION

High pathogenicity avian influenza (HPAI) A/H5Nx viruses continue to expand across continents and hosts with incursions into mammals and sporadic spillovers in humans.[1–7] H5 viruses have diverged extensively in wildlife, giving rise to multiple clades across both avian and mammalian hosts.[1,2,5] These dynamics in nature have driven rapid antigenic diversification, emergence of novel neuraminidase (NA) reassortants, and human infections with strikingly different case fatality rates (CFRs).[7–10] The current 2.3.4.4b panzootic has resulted in only 3 deaths from 97 cases (3% CFR), whereas the genetically distinct clade 2.3.2.1e viruses circulating in Southeast Asia have produced human infections with CFRs exceeding 50% over the past two years.[8–10] Such variability reflects the exceptional evolutionary plasticity of the H5 hemagglutinin (HA) and the increasing frequency of NA and internal-gene reassortment events driven by cross-species transmission (Figure 1A). These processes generate a multidimensional and rapidly shifting antigenic landscape that challenges strain-matched vaccine

This is an open access article under the CC BY license (http://creativecommons.org/licenses/by/4.0/).

Please cite this article in press as: Del Rosario et al., Broad vaccine protection against globally diverse influenza A/H5Nx viruses, Cell Reports Medicine (2026), https://doi.org/10.1016/j.xcrm.2026.103131

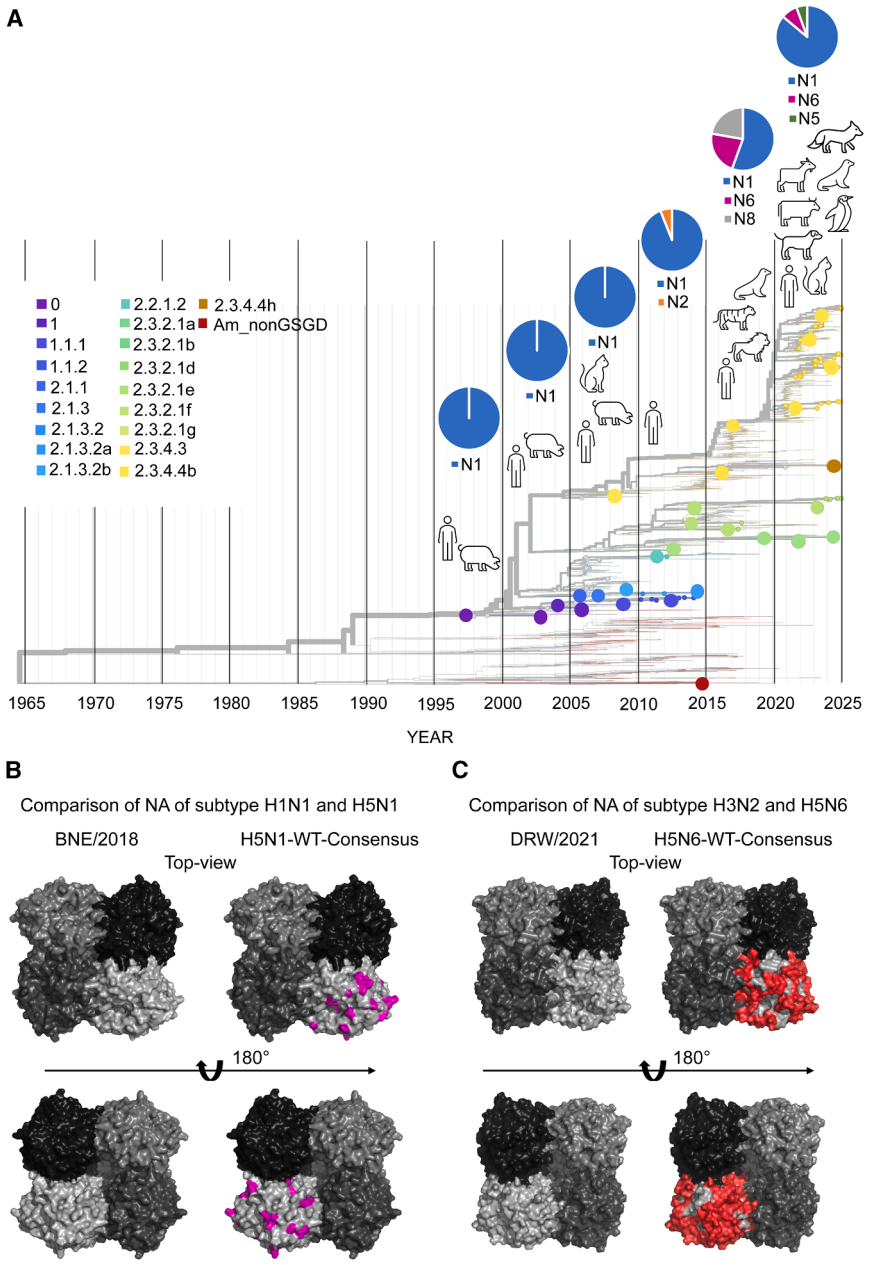


Figure 1. Evolutionary trajectory of HA and NA of H5Nx viruses

(A) A timetree[11] representing the temporal evolution of A/H5Nx in humans and mammals was generated from Nextstrain[12] using 137 sequences from GISAID[13–15] (Table S1). Nodes of the tree are color-coded according to GISAID clade assignments. Pie charts represent the fraction of reassorted NA subtypes observed in the dataset in the time frame (5 years) bound by thick vertical lines with hosts represented as icons. A subset of hosts for time frame 2021–2025 is shown for clarity. (B) Surface representations comparing the N1 from H1N1 A/Brisbane/02/2018 (BNE/2018), and consensus N1 from H5N1 strains based on A/mute swan/England/053054/2021 (mu/ENG/2021), A/harbor seal/Maine/22-020983-007-original/2022 (ha/ME/2022), A/mink/China/CY/2017 (mi/CHN/2017), and A/British Columbia/PHL-2032/2024 (BC/2024). The ectodomain of NA is represented as a gray surface with mutations between N1 from H1N1 and N1 from H5N1 highlighted in magenta. Sequence alignments for these comparisons are in Figure S1A. (C) Surface representations comparing the NA of H3N2 A/Darwin/9/2021 (DRW/2021), and consensus N6 from H5N6 strains based on A/Sichuan/26221/2014 (SC/2014), A/Anhui/2021_00011/2020 (AN/2020), and A/duck/NgheAn/5382VTC/2019 (du/NgheAn/2019). The ectodomain of NA is represented as a gray surface with mutations between N2 from H3N2 and N6 from H5N6 highlighted in red. Sequence alignments for these comparisons are in Figure S1B.

The surface images of neuraminidase were rendered using Pymol version 2.5.0 (The PyMOL Molecular Graphics System, version 3.0, Schrödinger, LLC.) using PDB: 7S0I[16] and 5HUM,[17] respectively.

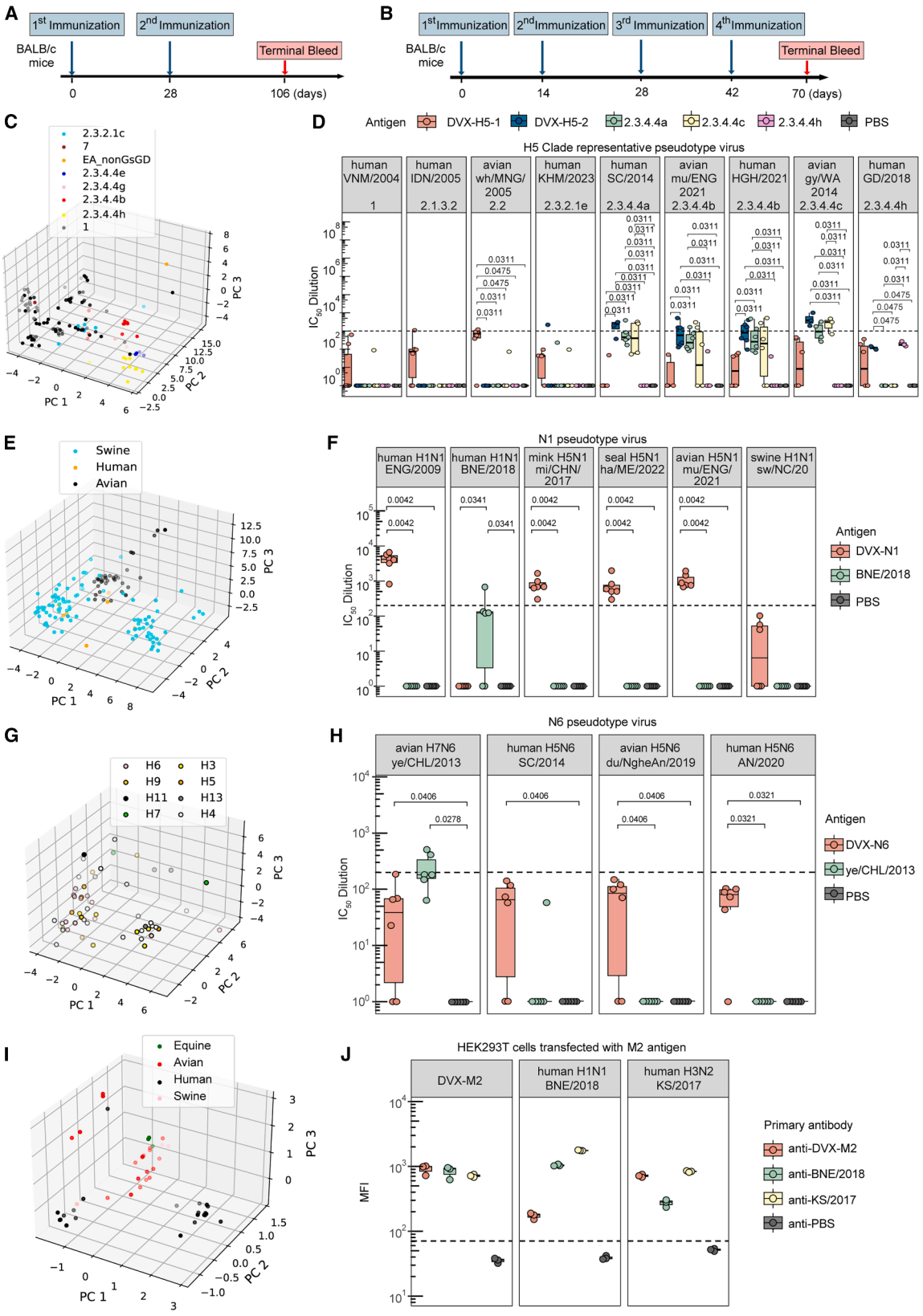
strategies anchored to static representations of a moving target.

While clade 2.3.4.4b viruses currently dominate western hemisphere epizootics,[1,2,5,18] multiple H5 clades, including clade 2.3.2.1e, circulate and evolve independently across Asia, Europe, and Africa.[5,8,18] These viruses occupy ecological niches and accumulate mutations under host-adaptation pressures, producing HA and NA antigen-evolution trajectories that are distinct[19] and cannot be captured by a single strain-specific immunogen. Reassortment with other goose/Guangdong (Gs/Gd) lineage viruses and local low pathogenicity avian influenza (LPAI) strains have further diversified NA and other internal genes, with consequences for receptor binding, replication efficiency, host tropism, and transmissibility.[2,6,20] As a result, the next zoonotic spillover capable of human-to-human transmission may differ antigenically from any existing vaccine candidates. These evolutionary dynamics intersect with the variety of human immunological backgrounds. For example, pre-existing immunity from seasonal H1N1 infections can confer partial protection against some H5 viruses through conserved HA stalk epitopes[21–25] and shared N1 antigenicity (Figures 1B and S1A).[26–30] This may in part explain why H5N1 clade 2.3.4.4b viruses that adapted to dairy cattle in the United States have caused only predominantly mild human disease despite high-risk exposure.[5,31–34]

Additionally, NA-directed immunity provides a mechanistic counterbalance to HA-driven diversification. NA-specific antibodies can restrict viral egress, reduce viral burden, and accelerate recovery even when HA-directed immunity is mismatched.[26–30,35,36] Among NA-reassorted H5 viruses in humans (Figure 1A), H5N6 is particularly concerning. Humans possess limited or no pre-existing immunity to this NA subtype,

Please cite this article in press as: Del Rosario et al., Broad vaccine protection against globally diverse influenza A/H5Nx viruses, Cell Reports Medicine (2026), https://doi.org/10.1016/j.xcrm.2026.103131

CellPress
OPEN ACCESS



(legend on next page)

Please cite this article in press as: Del Rosario et al., Broad vaccine protection against globally diverse influenza A/H5Nx viruses, Cell Reports Medicine (2026), https://doi.org/10.1016/j.xcrm.2026.103131

evidenced by H5N6 infections exhibiting the highest CFR (>50%) among group-2 NA reassorted viruses.[8,37–39] Although immune memory from historical N2 exposure (e.g., H2N2 and H3N2 infections in humans) can confer partial protection against some N2-bearing viruses,[40] the substantial divergence between N2 and N6 (Figures 1C and S1B) reduces the likelihood of meaningful antigenic cross-protection, making H5N6 a unique, under-addressed threat within the H5Nx landscape.

These factors highlight the limitations of strain-specific HA-centric vaccines, including consensus or "centralized" HA immunogens[41] and the need for strategies that anticipate antigenic diversification. Strain-matched clade 2.3.4.4b vaccines that are authorized for use in case of a pandemic have not been extensively tested for cross-protection against viruses from circulating H5 clades.[42–46] To address this, we engineered a broadly protective, multi-antigen panH5Nx vaccine using computational and structure-guided HA, NA, and M2 antigens, capturing global H5Nx diversity. The resulting DVX-panH5Nx multi-antigen mRNA-LNP vaccine combines complementary mechanisms of HA-mediated entry neutralization, NA-mediated egress restriction, and M2-mediated immune potentiation to deliver robust protection resilient to HA clade differences and NA reassortment. Here, we evaluate DVX-panH5Nx in mice and ferrets and benchmark its performance against WHO whole-inactivated candidate vaccine viruses (CVVs). Together, these data demonstrate a pre-pandemic H5 vaccine approach that aligns with host-pathogen biology and addresses the practical constraints of outbreak response.

RESULTS

In silico design of digitally engineered HA, NA, and M2 antigens

To engineer antigen candidates capturing both conserved and representative variable epitopes across globally circulating H5Nx viruses, we used Digitally Immune-Optimized Synthetic vaccine (DIOSynVax)[47,48] technology. Evolutionary modeling identified antigen candidates with minimal phylogenetic distance to their corresponding global sequence datasets compiled using the GISAID[13–15] and NCBI[49] databases, ensuring broad representation of circulating HA, NA, and M2 diversity. Two engineered H5 antigens were generated; DVX-H5-1 from all globally distributed clades that have caused human infection and DVX-H5-2 from the rapidly evolving clade 2.3.4.4 (Figures 2C and S2A). Engineered N1 (DVX-N1) (Figures 2E and S1A) and N6 (DVX-N6) (Figures 2G and S1B) NAs were derived from non-redundant datasets encompassing human, avian, and mammalian isolates. A broadly representative M2 antigen (DVX-M2) (Figure 2I, Data S2B) was designed from human, avian, swine, and equine influenza A sequences. Antigens were then functionally validated *in vitro* by pseudotyping lentiviruses with DVX-H5-1 (Figure S3A), DVX-H5-2 (Figure S3B), DVX-N1, and DVX-N6 antigens (Figure S3C). The DVX-H5 pseudotype viruses (PVs) were neutralized by a panel of monoclonal antibodies against HA (Figures S3A and S3B), while the DVX-N1 and DVX-N6 PVs demonstrated NA activity by cleaving fetuin (Figure S3C). Functional validation of each antigen confirmed that the engineered HA pseudotypes were identified by conformation-dependent monoclonal antibodies, and engineered NA pseudotypes exhibited robust enzymatic activity (Figure S3).

Individual candidate antigens are immunogenic in BALB/c mice

To evaluate immunogenicity, groups of BALB/c mice were immunized (Figures 2A and 2B) with one of the following DNA antigens, DVX-H5-1 and DVX-H5-2 (Figure 2D), DVX-N1 (Figure 2F), DVX-N6 (Figure 2H), and DVX-M2 (Figure 2J), listed in Table S2A. DNA plasmids encoding sequences representative of wild-type strains were included as comparators. The wild-type strains for H5 were selected based on CVVs. N1 and M2 controls

Figure 2. Computationally designed DVX DNA antigens are immunogenic in mice

(A) Immunization and bleed schedule of mice immunized with DVX-H5-1, DVX-H5-2, and controls, and (B) DVX-N1, DVX-N6, DVX-M2, and controls as stated in Table S2A.

(C) Principal component (PC) plot showing non-redundant dataset of hemagglutinin H5 sequences from A/H5 clades used as input for generation of DVX-H5-1, and DVX-H5-2. Each dot represents a full-length HA amino acid sequence and is color-coded according to the clade they belong to.

(D) BALB/c mice were immunized with DVX-H5 antigen candidates and wild-type controls. Neutralizing titers as shown by terminal bleed serum IC_{50} (half-maximal dilution resulting in 50% neutralization) values against A/H5 pseudotype viruses (PVs) (Table S3A) representing relevant A/H5 clades. Dashed line indicates an IC_{50} of 10^3, a threshold for a predicted protective immune response in a pseudotype neutralization assay (pMN).[47,50–52]

(E) PC plot showing a non-redundant dataset of neuraminidase N1 sequences used as input for generation of DVX-N1. Each dot represents a full-length N1 amino acid sequence and is color-coded according to the host species. Sequences are predominantly from H1N1 and H5N1 virus strains.

(F) BALB/c mice were immunized with DVX-N1 and wild-type control BNE/2018. Inhibition of N1 PV (Table S3B) from terminal bleeds are shown as IC_{50} dilution values determined using the pseudotype enzyme-linked lectin assay (pELLA). Dashed line indicates an IC_{50} of 200, the predicted baseline for an effective neuraminidase inhibition response.[53]

(G) PC plot showing a non-redundant dataset of neuraminidase N6 sequences used as input for generation of DVX-N6. Each dot represents a full-length N6 amino acid sequence and is color-coded according to the HA it partners with.

(H) BALB/c mice were immunized with the DVX-N6 antigen candidate and wild-type control ye/CHL/2013 (N6). Inhibition of N6 PVs (Table S3B) from terminal bleeds are shown as IC_{50} dilution values determined via pELLA.

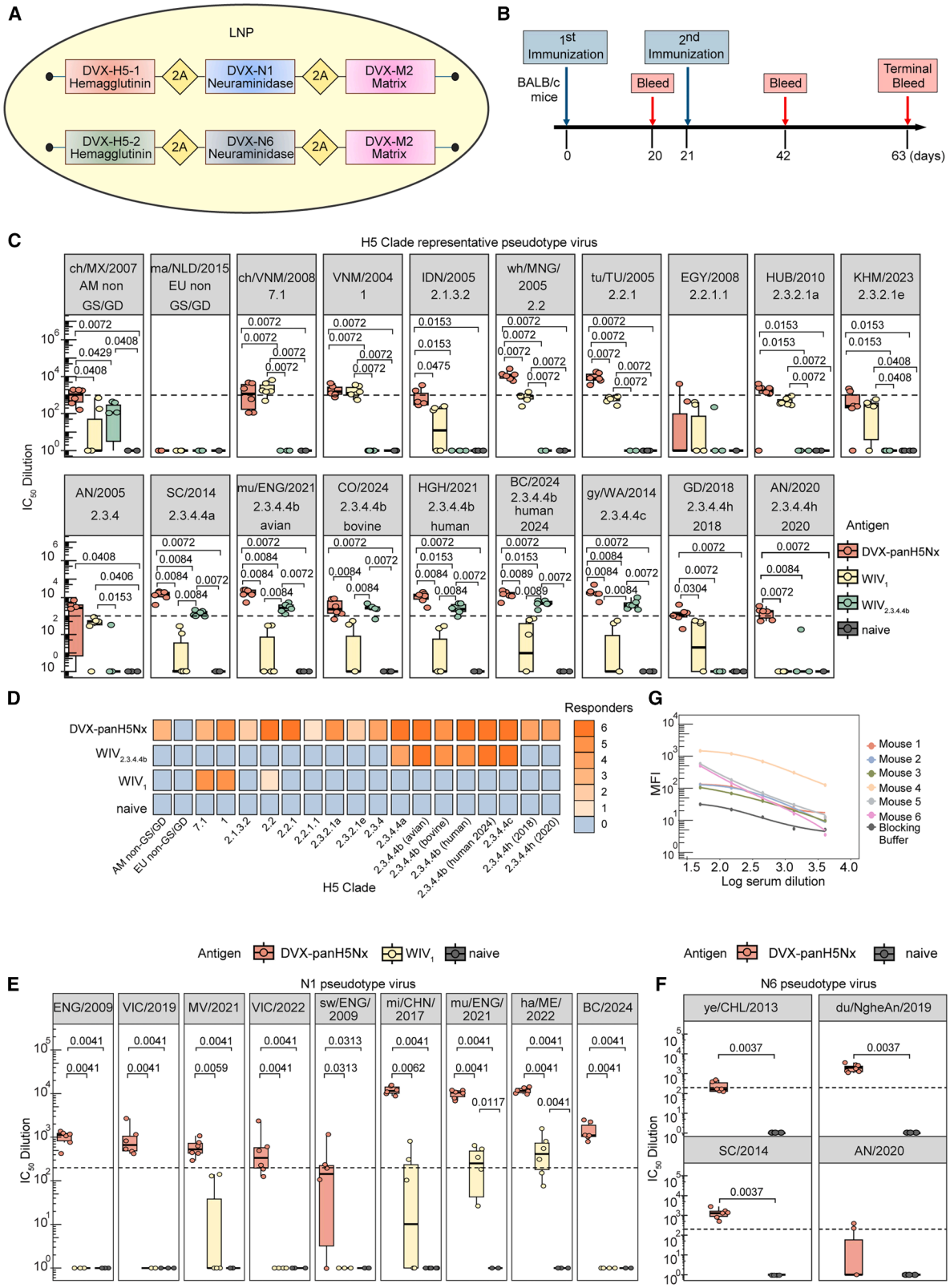
(I) PC plot showing a non-redundant dataset of matrix protein 2 (M2) IAV sequences used as input for generation of DVX-M2. Each dot represents a full-length M2 amino acid sequence and is color-coded according to the host species.

(J) BALB/c mice were immunized with DVX-M2 antigen candidate and M2 wild-type controls from BNE/2018 (H1N1) and KS/2017 (H3N2) (Table S3C). Binding of terminal sera from immunized mice to HEK293T cells transfected with DVX-M2 and wild type controls is reported as median fluorescence intensity (MFI) values (*y* axis). For each serum sample, three replicates are reported. Dotted line indicates the limit of detection (LOD) of the assay.

For (D), (F), (H), and (J), the median and interquartile range of individual mouse serum samples are shown ($n = 6$/immunization group). Only statistically significant comparisons ($p < 0.05$) determined by Wilcoxon rank test with Benjamini-Hochberg correction are indicated.

Please cite this article in press as: Del Rosario et al., Broad vaccine protection against globally diverse influenza A/H5Nx viruses, Cell Reports Medicine (2026), https://doi.org/10.1016/j.xcrm.2026.103131

CellPress
OPEN ACCESS



(legend on next page)

were selected based on strains previously used in the seasonal flu vaccine. The N6 control was selected as it was the most phylogenetically distant to DVX-N6.

Immunogenicity was poor ($IC_{50} < 10^3$) in all antigens against clades 1, 2.1.3.2, 2.2, and 2.3.2.1e; nonetheless, at least 4/6 mice immunized with DVX-H5-1 seroconverted and elicited higher neutralization titers against PVs from clade 2.1.3.2 and clade 2.2 (Figure 2D). These numbers were higher compared to the rest of the groups. Mice immunized with DVX-H5-2 seroconverted to all clade 2.3.4.4 PV with no significant difference in titers observed with mice immunized with HA wild-type controls (Figure 2D). Among the wild-type HA controls, only the homologous 2.3.4.4h clade HA neutralized the 2.3.4.4h PV, with wild-type HA from 2.3.4.4a and 2.3.4.4c showing no response. Although potency was below the threshold for all immunization groups, these findings indicate that DVX-H5-1 and DVX-H5-2 still elicited broader responses than the controls.

All mice immunized with DVX-N1 generated NA inhibition titers against all N1 PV of human, avian, and mammalian origin except for BNE/2018 (Figure 2F). The wild-type control human BNE/2018-immunized mice inhibited homologous NA but not any other tested PV. Similarly, at least 4/6 mice immunized with DVX-N6 inhibited all PV tested of human and avian origin; while the wild-type N6 control avian ye/CHL/2013 inhibited only the homologous strain but not any other PV (Figure 2H). These data support the wider breadth of our DVX-NA antigens compared to selected wild-type N1 and N6 antigens.

Mice immunized with DVX-M2 generated binding titers ($MFI > 10^2$) against cells expressing the homologous antigen DVX-M2 and M2 proteins from human BNE/2018(H1N1) and KS/2017(H3N2) (Figure 2J). However, no significant differences between DVX-M2 and the M2 of wild-type strains were observed.

Superior cross-clade neutralization of DVX-panH5Nx compared to whole inactivated wild-type virus-based antigens in mice

Within the last decade, mRNA vaccine technology combined with new generations of lipid nanoparticles (LNPs) has proven to be highly immunogenic and rapidly scalable in the event of an outbreak.[54–58] Taking advantage of these advancements and to improve immunogenicity, we converted our best in class engineered antigens into two mRNA antigen "strings" linked by 2A peptide sequences,[59] with DVX-H5-1_DVX-N1_DVX-M2 as the first string and DVX-H5-2_DVX-N6_DVX-M2 as the second string. The two mRNA strings were formulated at equal molar proportions as a single LNP preparation designated DVX-panH5Nx (Figures 3A; Figures S4A and S4B). The polycistronic expression of all three HA, NA, and M2 antigens from the same transcript ensures their co-expression within the same transfected cell. Immunogenicity of DVX-panH5Nx was benchmarked against whole inactivated virus (WIV) vaccines based on WHO-recommended CVVs from clades 1 and 2.3.4.4b that have been pre-authorized for human use in the event of a human H5 influenza outbreak (Table S2B).

Day 63 (D63) sera (Figure 3B) revealed neutralization responses across an H5 PV panel from different clades that are phylogenetically and antigenically distinct from each other, including strains that caused bovine infections and outbreaks in Colorado[60] and the recent H5N1 clade 2.3.4.4b (genotype D.1.1) virus that caused a severe infection in an adolescent in British Columbia.[61] Neutralizing titers (IC_{50}) $\geq 10^3$ (an arbitrary potency threshold in our standardized pMN assay[47,50–52]) were observed in mice immunized with DVX-panH5Nx against PV from the American non-Gs/Gd lineage and Gs/Gd clades 7.1, 1, 2.1.3.2, 2.2, 2.2.1, 2.3.2.1a, 2.3.2.1e, 2.3.4.4a, 2.3.4.4b, 2.3.4.4c, and 2.3.4.4h (Figure 3C). Mice immunized with the CVV A/Vietnam/1194/2004 (H5N1) (WIV_1) developed $IC_{50} \geq 10^3$ only against clades 7.1 and 1, while those immunized with the CVV A/Astrakhan/3212/2020 (H5N8) ($WIV_{2.3.4.4b}$) developed titers against 2.3.4.4a, 2.3.4.4b, and 2.3.4.4c PV but not against 2.3.4.4h or the other clades tested. Neither of the WIVs reached the titer nor the cross-clade neutralization breadth exhibited by DVX-panH5Nx (Figure 3C). The number of mice that responded above the defined IC_{50} threshold is depicted as heatmaps in Figure 3D, demonstrating DVX-panH5Nx's superior immune breadth compared to the benchmark CVV whole inactivated vaccines.

NA inhibition of DVX-panH5Nx was in the range of $IC_{50} \sim 10^2$–10^4 against N1 from seasonal strains such as VIC/2019 and VIC/2022, pandemic strains ENG/2009 and sw/ENG/2009, and from multiple spillover species such as mink, avian, harbor seal, and the H5N1 case from British Columbia, a clade 2.3.4.4b D1.1 NA reassortant[30] (Figure 3E). Interestingly, WIV_1 (with an N1 component) induced inhibition titers to less than half of the N1 PV, with titers at least 100-fold lower than DVX-panH5Nx against all PVs tested. These data demonstrated the significantly superior responses induced by DVX-panH5Nx over WIV vaccines in terms of N1 inhibition. Additionally, DVX-panH5Nx elicited anti-N6 titers in the range of $IC_{50} \geq 10^3$ against avian N6, du/NgheAn/2019 (N6), and human SC/2014 (N6) and $IC_{50} \sim 10^2$

Figure 3. DVX-panH5Nx induces broad humoral responses in mice compared to CVV

(A) Composition of the mRNA panH5Nx vaccine candidate DVX-panH5Nx. DVX-panH5Nx is composed of two mRNA expression strings linked by 2A peptide sequences, (1) DVX-H5-1_DVX-N1_DVX-M2 and (2) DVX-H5-2_DVX-N6_DVX-M2. The two mRNA strings were formulated at equal molar proportions as a single LNP preparation.

(B) Immunization and bleed schedule of mice (Table S2B). Terminal bleeds from D63 were used in serological investigations.

(C) Serum neutralizing titers as shown by IC_{50} values determined by pMN against an H5 PV panel (Table S3A). Dashed line indicates an IC_{50} value of 10^3.

(D) Heatmap representation of neutralization titers of all immunization groups against H5 PV from indicated clades. Legend indicates total mouse responders with an $IC_{50} \geq 10^3$ for each group.

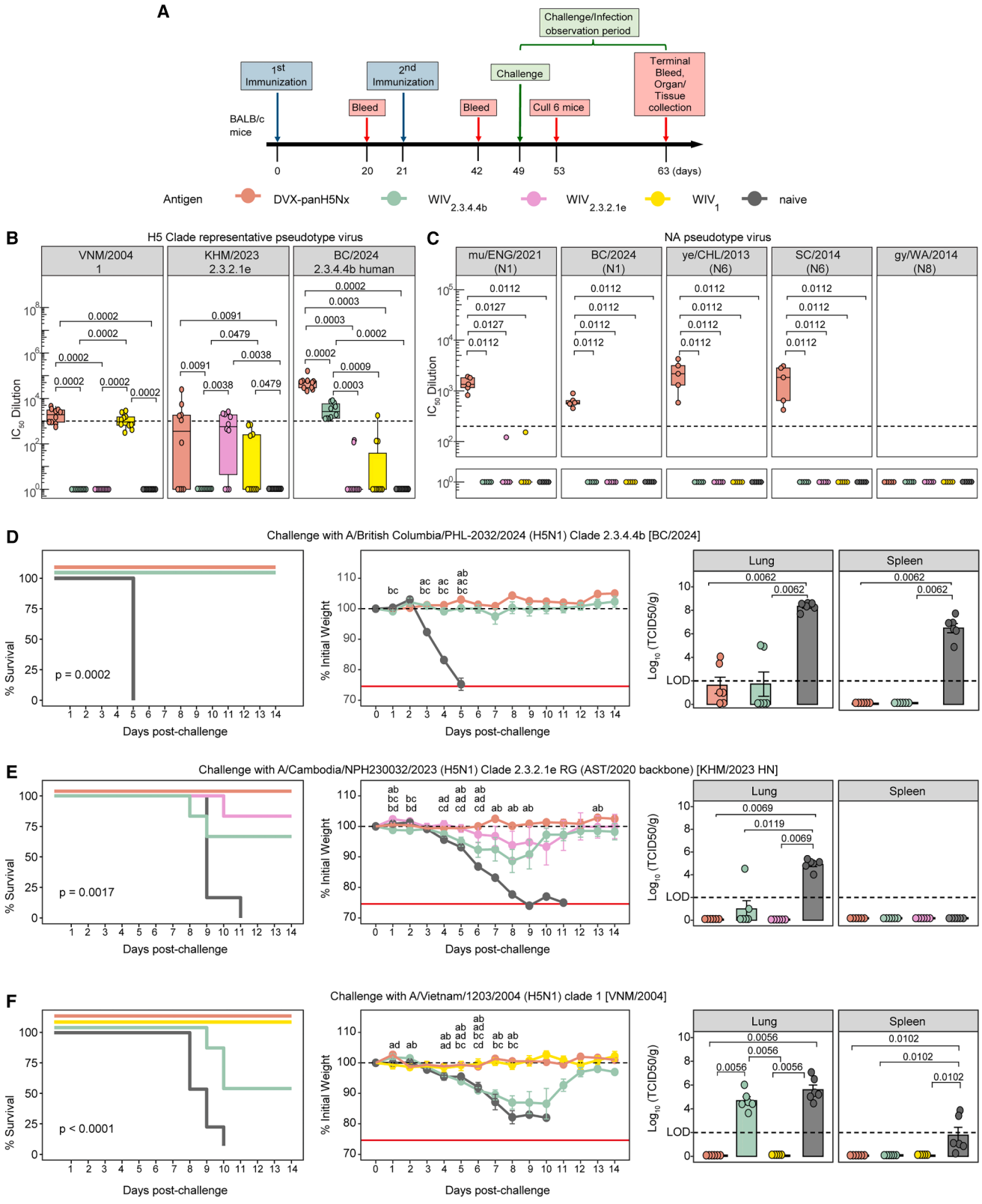
(E) NAI titers against N1 and (F) N6 PV panels (Table S3B) as shown by IC_{50} values determined by pELLA. Dashed line indicates an IC_{50} value of 200.

(G) Binding activity of M2-specific IgG antibodies, shown as MFI values, of serum from mice immunized with DVX-panH5Nx against recombinant M2 protein from A/chicken/Hebei/326/2005 (H5N1).

For (C), (E), and (F), the median and interquartile range of individual mouse serum samples are shown ($n = 6$/immunization group). Only statistically significant comparisons ($p < 0.05$) determined by Wilcoxon rank test with Benjamini-Hochberg correction are indicated.

Please cite this article in press as: Del Rosario et al., Broad vaccine protection against globally diverse influenza A/H5Nx viruses, Cell Reports Medicine (2026), https://doi.org/10.1016/j.xcrm.2026.103131

CellPress
OPEN ACCESS



(legend on next page)

Please cite this article in press as: Del Rosario et al., Broad vaccine protection against globally diverse influenza A/H5Nx viruses, Cell Reports Medicine (2026), https://doi.org/10.1016/j.xcrm.2026.103131

against avian ye/CHL/2013 (N6) (Figure 3F). Mice immunized with DVX-panH5Nx also generated binding antibodies against recombinant M2 protein from A/chicken/Hebei/326/2005 (H5N1) (Figure 3G). The protective role of M2 has been demonstrated by several independent studies,[62–65] and in the case of DVX-panH5Nx, it is hypothesized to potentiate immune responses directed at HA and NA.

Cross-clade efficacy of DVX-panH5Nx against lethal mouse H5N1 challenges

Following demonstration of immune breadth across A/H5 clades, the vaccine efficacy of DVX-panH5Nx was evaluated in mice. In parallel, mice were lethally challenged with viruses from three distinct H5N1 clades (clades 1, 2.3.2.1e, and 2.3.4.4b) that have caused human infections and thereby represent a potential pandemic threat (Figure 1A). Protection afforded by DVX-panH5Nx was compared to that of currently pre-authorized CVV-based vaccine for use in the event of an A/H5Nx human outbreak, A/Astrakhan/3212/2020 (H5N8) ($WIV_{2.3.4.4b}$), and the nearest CVV-based antigens (WIV_1, $WIV_{2.3.2.1e}$) to the respective challenge viruses (Table S2C).

All mice were immunized on D0 and D21 (Figure 4A). Only DVX-panH5Nx and WIV_1 demonstrated neutralization against clade 1 VNM/2004 (Figure 4B). Similarly, there was no significant difference in the neutralization titers of DVX-panH5Nx, $WIV_{2.3.2.1e}$, and WIV_1 against the clade 2.3.2.1e PV, KHM/2023. Sera from $WIV_{2.3.4.4b}$ mice did not neutralize the clade 1 and clade 2.3.2.1e PV. Against a 2.3.4.4b PV, BC/2024, both DVX-panH5Nx and $WIV_{2.3.4.4b}$ demonstrated $IC_{50} \geq 10^3$ while there was little to no neutralization from WIV_1 and $WIV_{2.3.2.1e}$ mice (Figure 4B). Moreover, only DVX-panH5Nx mice demonstrated NA inhibition titers against various N1 and N6 PV tested pre-challenge (Figure 4C). Although they have an N1 component, neither WIV_1 nor $WIV_{2.3.2.1e}$ inhibited any of the N1 tested. $WIV_{2.3.4.4b}$ also did not inhibit the N8 PV, gy/WA/2014. These findings reiterate the narrow strain-specificity (Figures 3C and 3D, 4B) and lack of NA inhibition potential (Figure 4C) of the WIVs.

At D49, mice were challenged and weight loss and clinical symptoms of infection were observed for 14 days or until mice were culled for reaching the humane endpoint (≥25% weight loss from initial). There was 100% survival in mice immunized with DVX-panH5Nx with no weight loss or clinical symptoms of influenza observed against any of the challenge viruses for the study duration, demonstrating complete protection by a single vaccine from multiple diverse clades of HPAI H5 viruses (Figures 4D–4F). In contrast, while animals immunized with the benchmark CVV-based $WIV_{2.3.4.4b}$ were protected against the 2.3.4.4b-matched challenge virus (Figure 4D), only 67% survived with weight loss and clinical symptoms commencing 5 days post-challenge (dpc) against 2.3.2.1e H5N1 (Figure 4E) and only 50% survived with weight loss observed as early as 4 dpc against clade 1 H5N1 challenge (Figure 4F). $WIV_{2.3.2.1e}$-immunized mice showed weight loss from 7 to 11 dpc with 83% survival against the 2.3.2.1e challenge (Figure 4E), while all WIV_1-immunized mice survived the clade 1 challenge (Figure 4F). In all challenges, mice from the naive group developed disease and were culled due to reaching humane endpoints as early as 5 dpc (Figures 4D–4F).

Virus titers in lung and spleen collected at 4 dpc were below the limit of detection (LOD) in mice immunized with DVX-panH5Nx (Figures 4D–4F, third image). In contrast, virus could be detected in the lungs of $WIV_{2.3.4.4b}$ mice challenged with clade 1 H5N1 (Figure 4F, third image), in the lungs of naive mice against all challenge viruses (Figures 4D–4F, third image), and 2.3.4.4b virus was also detected in their spleens (Figure 4D, third image). This evidence suggests that DVX-panH5Nx protects mice against lethal challenge of divergent H5N1 viruses by limiting viral replication in the lungs, thereby controlling infection and correlating with survival.

DVX-panH5Nx induces broad H5 neutralization and NA inhibition in ferrets

We then evaluated DVX-panH5Nx vaccine efficacy in ferrets, a well-characterized model of human influenza infection,[66,67] in comparison to the adjuvanted CVV-based whole inactivated A/Astrakhan/3212/2020 (H5N8) ($WIV_{2.3.4.4b}$). Additionally, we administered a lower dose of DVX-panH5Nx in a second LNP, designated DVX-panH5Nx_FML2. All ferrets were immunized using the same schedule used to evaluate immunogenicity in mice (Figure 5A; Table S2D), with DVX-panH5Nx given at a high dose of 100 μg and DVX-panH5NX_FML2 at a low dose of 25 μg. Additionally, supporting HA-neutralization data from a separate long-interval study in mice, in which both DVX-panH5Nx_FML2 and $WIV_{2.3.4.4b}$ groups received two immunizations, are shown in Figures S4C–S4F.

Hemagglutination inhibition (HI) demonstrated comparable HI titers in all immunized groups (Figure 5B). DVX-panH5Nx elicited

Figure 4. DVX-panH5Nx protects against diverse viruses representing over 20 years of H5Nx evolution with greater efficacy over A/H5 CVV strain-based vaccines

(A) Study schedule of mice immunized with DVX-panH5Nx and control vaccines (Table S2C).

(B) HA-serum neutralizing titers on D42 pre-challenge as shown by IC_{50} values determined by pMN against the closest H5 PV to the WIV controls from immunized mice. Dashed line indicates an IC_{50} value of 10^3.

(C) NAI titers against selected N1, N6, and N8 PV (Table S3B) as shown by IC_{50} values determined by pELLA. Dashed line indicates an IC_{50} value of 200.

(D–F) Mice were challenged with (D) A/British Columbia/PHL-2032/2024 (H5N1) (clade 2.3.4.4b) [BC/2024], (E) A/Cambodia/NPH230032/2023 (H5N1) (clade 2.3.2.1e) [KHM/2023 HN], and (F) A/Vietnam/1203/2004 (H5N1) (clade 1) [VNM/2004]. (D–F, first image) Kaplan-Meier survival curves with *p* value indicating the result of Log Rank (Mantel-Cox) test. (D–F, second image) Average weights as monitored for all immunization groups for 14 days and changes to initial weight indicated as % on the *y* axis. Weights with statistically significant differences as determined by unpaired t-tests with Benjamini Hochberg correction are indicated by letters, with *p* values summarized in Table S4A. The red line at 75% indicates the humane endpoint of the study. (D–F, third image) Tissue culture 50% infectious dose ($TCID_{50}$) values per gram of lung and spleen tissue from mice culled at 4 dpc.

Plots show the median and interquartile range of individual mouse serum samples. Only statistically significant comparisons ($p < 0.05$) determined by Wilcoxon rank test with Benjamini-Hochberg correction are indicated. For all images, $n = 6$ mice/group.

Please cite this article in press as: Del Rosario et al., Broad vaccine protection against globally diverse influenza A/H5Nx viruses, Cell Reports Medicine (2026), https://doi.org/10.1016/j.xcrm.2026.103131

CellPress
OPEN ACCESS

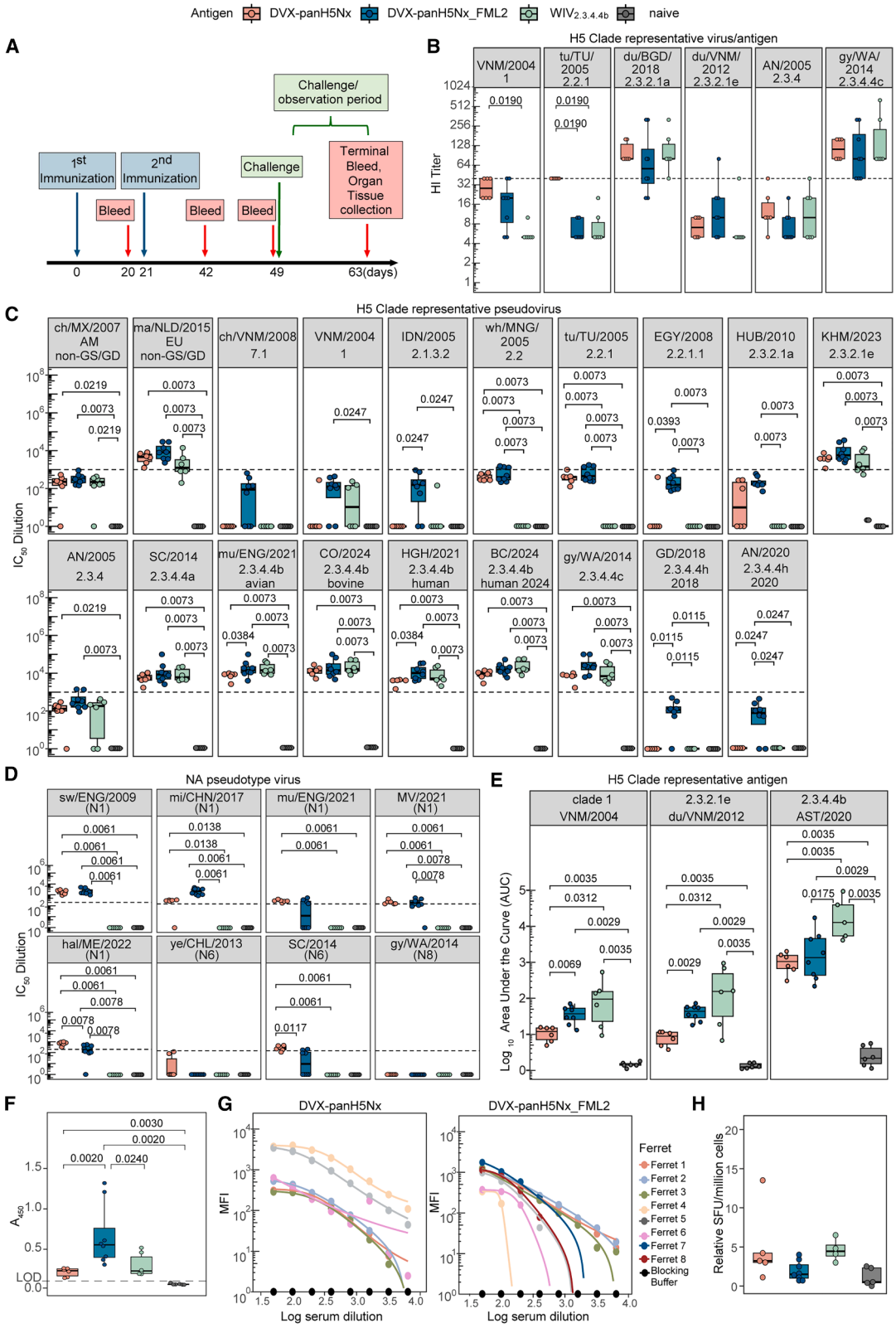


Figure 5. DVX antigens demonstrate broad immunogenicity in ferrets

(A) Study schedule of ferrets immunized with DVX-panH5Nx, DVX-panH5Nx_FML2 (a dose-sparing formulation), and controls (Table S2D). Bleeds taken on D42 were used for all serological assays. Ferrets were challenged on D49 with HPAI A/chicken/Italy/23VIR3799-1/2023 (H5N1), a clade 2.3.4.4b H5N1 virus.

(legend continued on next page)

4 to 10-fold higher HI titers to viruses from clades 1 and 2.2.1, and a 2-fold increase against 2.3.2.1e compared to $WIV_{2.3.4.4b}$, consistent with data from mice, confirming the breadth of cross-protection induced by DVX-panH5Nx compared to the relatively narrow specificity of $WIV_{2.3.4.4b}$ (Figure 5B).

DVX-panH5NX_FML2 induced higher IC_{50} among immunized groups against all H5 PV tested (Figure 5C). There was a significant difference in neutralization of clades 2.2, 2.2.1, 2.2.1.1, and 2.3.2.1e between DVX-panH5Nx_FML2 and adjuvanted $WIV_{2.3.4.4b}$, where the latter showed no detectable activity. As expected, all groups except for naive animals induced considerable serum neutralization ($IC_{50} \sim 10^4$) against all clade 2.3.4.4 PV tested. DVX-panH5NX_FML2 and $WIV_{2.3.4.4b}$-immunized groups showed higher responses than DVX-panH5Nx ferrets with only DVX-panH5NX_FML2 ferrets inducing neutralizing titers against subclade 2.3.4.4h (Figure 5C). There was no significant difference in NA inhibition ($IC_{50} \geq 10^2$) for DVX-panH5Nx and DVX-panH5NX_FML2 against majority of N1 and N6 PV tested (Figure 5D). Despite having an N8 component, sera from adjuvanted $WIV_{2.3.4.4b}$ ferrets failed to inhibit the N8 PV (Figure 5D).

All immunized animals seroconverted with DVX-panH5Nx_FML2 and $WIV_{2.3.4.4b}$ showing significantly higher antibody binding titers compared to other groups (Figures 5E and 5F). Additionally, M2-specific IgG binding antibodies were detected in the DVX-panH5Nx and DVX-panH5NX_FML2 groups (Figure 5G).

The induction of T cell responses was also evaluated and representative IFN-γ ELISpot results for both DVX and adjuvanted WIV groups revealed greater IFN-γ spot-forming units (SFUs) compared to naive controls. However, no significant differences in SFU were observed among immunization groups (Figure 5H).

Together, these results mirrored previous findings in mice and demonstrated that DVX-panH5Nx in different LNPs at both low and high doses induced robust B cell responses including broad neutralization across diverse H5 clades, including N1 and N6 inhibition, together with T cell responses, consistent with the design criteria of these computationally generated DIOSynVax antigens.

DVX-panH5Nx vaccine candidates elicit superior efficacy against HPAI 2.3.4.4b challenge compared to CVV-based $WIV_{2.3.4.4b}$ in ferrets

Vaccine efficacy in ferrets was then assessed by lethal challenge with A/chicken/Italy/23VIR3799-1/2023 (H5N1), a representative of the current 2.3.4.4b panzootic, containing a 4-amino acid difference in the HA with $WIV_{2.3.4.4b}$ (Figure S5A). All naive control ferrets, and 50% of animals immunized with adjuvanted $WIV_{2.3.4.4b}$, reached clinical endpoint or succumbed to disease by 8 dpc. In contrast, all DVX-panH5NX_FML2 animals survived (100%), and only 1 DVX-panH5Nx animal reached the humane endpoint (Figure 6A). There was no weight loss or change in temperature in the DVX-panH5NX_FML2 ferrets, minimal weight loss and higher temperatures in DVX-panH5Nx animals, and significant weight loss from 6–8 dpc and minor temperature fluctuations in adjuvanted $WIV_{2.3.4.4b}$ animals (Figures 6B and 6C). Moreover, DVX-panH5Nx_FML2 ferrets showed little to no signs of infection with the lowest clinical scores on 7–10 dpc, the peak of infection. Ferrets immunized with DVX-panH5Nx achieved lower clinical scores relative to adjuvanted $WIV_{2.3.4.4b}$ and naive groups during the monitoring window, with clinical disease severity peaking for adjuvanted $WIV_{2.3.4.4b}$ ferrets 7–9 dpc (Figures 6D and S5B). All survivors had improved clinical outcomes reflected by less weight loss and lower clinical scores (Figures 6A–6D; Figure S5B). Competition ELISA demonstrated the presence of antibodies against the H5 HA of the Influenza A virus in all immunization groups and that these binding titers were significantly different from naive (Figure S5C).

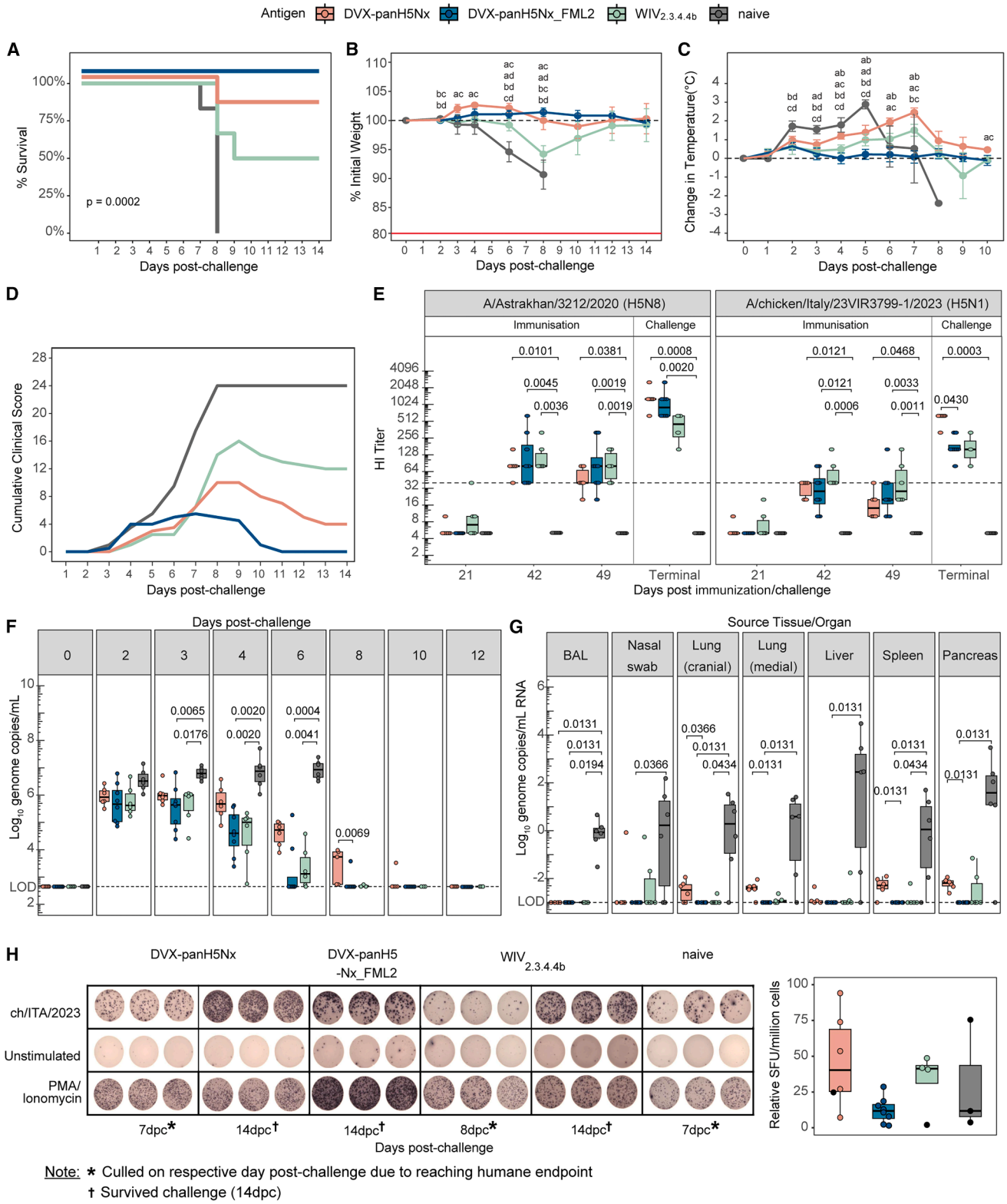
We then monitored HI titers at 21, 42, and 49 days post-immunization (dpi) to determine if clinical outcomes correlated with HI titers. Peak responses were observed 42 dpi in all groups except for naive, with the DVX and $WIV_{2.3.4.4b}$ groups all having HI $\geq$ 40 against A/Astrakhan/3212/2020 (homologous to the benchmark adjuvanted CVV $WIV_{2.3.4.4b}$); while lower titers were observed against the challenge virus (Figure 6E). However, $WIV_{2.3.4.4b}$, DVX-panH5NX_FML2, and DVX-panH5Nx groups showed decreased HI titers ~1:40, 1:20, and 1:15, respectively, on 49 dpi against the challenge virus, with the DVX groups all below the HI protective threshold (Figure 6E). As expected, all groups except for naive controls demonstrated seroprotective HI titers (HI $\geq$ 40) post-challenge. Nonetheless, survival of ferrets from both DVX groups suggest that correlates of protection other than HI titers impacted vaccine efficacy.

Additionally, there was no significant difference in viral shedding between DVX-panH5NX_FML2 and $WIV_{2.3.4.4b}$ ferrets (Figure 6F). Interestingly, despite superior clinical protection, shedding was observed in DVX-panH5Nx ferrets from 2–8 dpc compared to the $WIV_{2.3.4.4b}$ animals, while in naive disease progressors, viral

(B) Hemagglutination inhibition (HI) titers of sera from immunized ferrets against an H5 virus panel (Table S3D) representing various A/H5 clades. HI titers are expressed as the highest dilution of serum that inhibited hemagglutination completely. Dashed line indicates an HI titer of 40, the accepted threshold for a seroprotective response in this assay.
(C) Serum neutralizing titers as shown by IC_{50} values determined by pMN against an H5 panel (Table S3A). The dashed line indicates an IC_{50} value of 10^3.
(D) NAI titers against N1 and N6 (Table S3B) PV panels are shown as IC_{50} values determined by pELLA. Dashed line indicates an IC_{50} value of 200.
(E) Strain-specific binding antibodies against antigens from relevant H5 clades (Table S3E) were confirmed by ELISA. The *y* axis represents the logarithm of area under the curve (AUC) values from dose-response curves.
(F) Indirect ELISA to detect H5 binding antibodies in ferret serum samples against recombinant H5 hemagglutinin shown as Absorbance values at 450 nm (*y* axis) against A/H5 as detected via an ID Screen® Influenza H5 Indirect ELISA.
(G) Binding antibodies detected via Luminex shown as median fluorescence intensity (MFI) values against commercial recombinant M2 protein from A/chicken/Hebei/326/2005 (H5N1).
(H) IFN-γ secretion after PBMC stimulation with inactivated A/chicken/Italy/23VIR3799-1/2023 (H5N1) [ch/ITA/2023] is shown as relative spot-forming units (SFUs)/million cells.
All plots except (A) show the median and interquartile range for individual ferrets (n = 6 in DVX-panH5Nx, $WIV_{2.3.4.4b}$, and naive; n = 8 in DVX-panH5NX_FML2). Only statistically significant comparisons ($p < 0.05$) determined by Wilcoxon rank test with Benjamini-Hochberg correction are indicated.

Please cite this article in press as: Del Rosario et al., Broad vaccine protection against globally diverse influenza A/H5Nx viruses, Cell Reports Medicine (2026), https://doi.org/10.1016/j.xcrm.2026.103131

CellPress
OPEN ACCESS



Note: * Culled on respective day post-challenge due to reaching humane endpoint
† Survived challenge (14dpc)

Figure 6. Superior efficacy of DVX-panH5Nx in ferrets

(A) Kaplan-Meier survival curves for all immunization groups during the 14-day challenge window. *p* value indicates the result of log rank (Mantel-Cox) test among all groups.

(legend continued on next page)

RNA copies remained high until culling. Postmortem samples from bronchoalveolar lavages (BAL), lung, liver, spleen, and pancreas, demonstrated viral genome numbers below the LOD in all survivors indicating that immunizations halted viral multi-organ spread (Figure 6G). Infectious virus titers recovered from ferret lung homogenates post-challenge from all immunization groups were significantly different from naive (Figure S5D).

Compared to pre-challenge (Figure 5H), T cell responses increased in survivors (14 dpc) from all immunized groups post-challenge (Figures 6H and S6), suggesting that robust effector immune responses facilitated viral clearance. Interestingly, there were significantly lower SFUs detected in the DVX-panH5NX_FML2 ferrets, all of which survived challenge. Additionally, histopathology revealed a spectrum of lesions depending on the day of culling post-challenge. In general, animals with early progressive clinical disease (animals culled prior to the end of the monitoring window from $WIV_{2.3.4.4b}$ and naive groups) tended to have a higher degree of brain inflammatory infiltrates and/or more severe lung inflammation as opposed to animals that survived and had less severe interstitial changes (Table S5).

Together, this suggests that lower virus burden was driven by the combination of effective virus neutralizing-HA and NA-inhibiting antibodies, reflecting clearance of infection possibly by virus-stimulated T cells post-challenge.

DISCUSSION

The ongoing global expansion and diversification of H5Nx influenza viruses have revealed major gaps in current preparedness strategies which continue to rely on stockpiling strain-matched, clade-specific vaccines. Even with rapidly scaled mRNA vaccine manufacturing, conventional strain-based vaccines are inherently susceptible to mismatch, particularly as new HA and NA constellations arise through reassortment and host-adaptation with sustained circulation in animal reservoirs. The increasing diversity across H5Nx and high CFR H5N6 and 2.3.2.1e viruses create unpredictable risks for zoonotic transmission and pandemic emergence.

Here, we present a mechanistically informed, digitally engineered mRNA vaccine, DVX-panH5Nx, designed to anticipate viral evolution rather than reacting to it with single isolate-based vaccines. By integrating HA, NA, and M2 antigens representing global H5Nx diversity, we demonstrated that broad, cross-clade protection could be achieved using a single vaccine formulation. This breadth exceeds that of stockpiled whole-inactivated CVVs even when HI titers are lower, highlighting the limitations of HI as a sole predictor of protection when NA-mediated effector functions contribute substantially to immunity.

The breadth of immunogenicity reflected complementary activity of engineered HA and NA components. DVX-HA antigens induced cross-clade neutralization extending to divergent strains. Concurrently, DVX-NA antigens generated potent inhibition against N1 and N6 subtypes across seasonal, zoonotic, and human case-associated isolates, far exceeding those elicited by whole-inactivated comparator vaccines. Moreover, the addition of M2 may limit viral replication and reduce the severity of illness in a real-world setting by promoting cell-mediated immunity.[68]

Furthermore, the broad immunogenicity of DVX-panH5Nx translated into complete protection against lethal heterologous challenges in mice (Figure 4) and superior survival in ferrets (Figure 6). Protection encompassed multiple antigenically distinct H5N1 clades spanning two decades of viral evolution, including contemporary distinct clades. WHO stockpiled whole-inactivated H5 CVVs provided full protection only against homologous challenge, and rapidly lost efficacy against heterologous clades, even with higher HI titers. In contrast, DVX-panH5Nx conferred consistent survival across clades, demonstrating the advantage of rational, global diversity informed vaccines and the limitations of single strain-based vaccines.

The efficacy of a dose-sparing formulation further suggests operational flexibility in outbreak response. The higher neutralizing activity observed with the lower dose DVX-panH5Nx_FML2 may reflect differences in LNP formulation, including the alternative ionizable lipid, as well as the administered dose. These variables were not independently controlled in the present study, and their respective contributions cannot therefore be distinguished. Additionally, post-challenge T cell responses in survivors support the role for cellular immunity in viral clearance with DVX-vaccinated ferrets, particularly in the dose-sparing LNP formulation, requiring less effector expansion, suggesting lower antigenic burden and superior early containment.

(B) Weights were monitored for all groups for 14 days and changes to initial weight are indicated in % on the *y* axis. Plot shows mean values with standard deviation. Weights with statistically significant differences as determined by unpaired t-tests are indicated by letters with *p* values summarized in Table S4B. The red line at 80% indicates the humane endpoint of the study.
(C) Rectal temperature was monitored for 14 days and changes to baseline temperature (0 dpc) are indicated on the *y* axis. Plot shows the mean ± SD. Rectal temperatures with statistically significant differences as determined by unpaired *t* tests are indicated by letters, with *p* values summarized in Table S4C.
(D) Cumulative clinical scores as recorded twice daily during the challenge window. Ferrets were scored from 0 to 4 with 0 given to ferrets with no symptoms and 4 to ferrets with severe symptoms resulting in culling.
(E) HI titer monitoring on days 21, 42, 49 dpi, and terminal of all vaccination groups against A/Astrakhan/3212/2020 (H5N8), and the challenge virus, A/chicken/Italy/23VIR3799-1/2023 (H5N1). Dashed line indicates an HI titer of 40.
(F) Shedding of viral RNA from nasal washes is indicated as $\log_{10}$ genome copies/mL on the *y* axis, with days post challenge (dpc) on the *x* axis. From 8 to 12 dpc, only surviving ferrets are presented. The LOD at 2.65 ($\log_{10}$ genome copies/mL) is indicated by a dashed line.
(G) Viral RNA in postmortem tissues and organs is indicated as genome copies/μL RNA on the *y* axis with dpc on the *x* axis. LOD is indicated by dotted line.
(H) IFN-γ secretion after stimulation with inactivated challenge virus (ch/ITA/2023) is shown as spot-forming unit (SFUs) from representative wells in an ELISpot (left). Relative SFU/million cells were also plotted (right).
For all plots, $n = 6$ ferrets/group; $n = 8$ for DVX-panH5NX_FML2. In (E)–(H), plots show the median and interquartile range for individual ferrets. Only statistically significant comparisons ($p < 0.05$) determined via Kruskal-Wallis test followed by post-hoc Dunn's test (E and F) and Wilcoxon test with Benjamini-Hochberg correction (G and H) are indicated.

Please cite this article in press as: Del Rosario et al., Broad vaccine protection against globally diverse influenza A/H5Nx viruses, Cell Reports Medicine (2026), https://doi.org/10.1016/j.xcrm.2026.103131

The DVX synthetic vaccine antigen design technology is complementary but different from the antigen-design approaches described by Kok et al.[41] that use antigenic cartography to identify an antigenically central HA within the known A(H5) antigenic landscape, a useful strategy for rationally selecting antigens that cover experimentally defined antigenic space. However, it remains dependent on the availability of HI titers, and is therefore constrained by viruses that have already been sampled and antigenically characterized, requiring continuous updating as new antigenic variants emerge. Alternatively, COBRA[69] technology generates broadly reactive influenza antigens by constructing computationally optimized consensus sequences across defined clades and time periods. This strategy has demonstrated utility for generating centralized influenza antigens. The resulting designs remain largely anchored to the sequence diversity included in the input dataset and are typically focused on defined viral subtypes or clades.

In contrast, the DIOSynVax pipeline uses curated sequence datasets together with phylogenetic and evolutionary modeling to design synthetic vaccine antigens that are not intended to reproduce a naturally occurring strain or a consensus sequence. Rather, our method seeks to incorporate evolutionarily informed features and phylogenetic relationships across divergent lineages to engineer synthetic antigens with broad protective potential to anticipate broader patterns of viral diversity.[48]

Compared with existing mRNA vaccines that pool separate HA antigens to confer immunogenicity, a single polycistronic mRNA-LNP simplifies the chemistry, manufacturing, and controls (CMC) aspect of vaccine development. Additionally, expression of all antigens from the same transcript ensures their co-expression within the same transduced cell, promoting coordinated trafficking through the secretory pathway and potentially enhancing presentation of multivalent membrane-bound antigen complexes. Importantly, the decision to include antigens other than HA has been shown here to trigger a strong immune response and target viral components that mutate less often than HA, providing a second line of defense in the case of HA mutant escape.

Together, these data support a shift in pandemic influenza preparedness toward broadly protective, digitally designed, multi-antigen vaccines that reflect global viral diversity. Leveraging genomic surveillance data from animal reservoirs and human spillover events, with structural insights and immune correlates, offers a powerful framework not only for next-generation pre-pandemic H5Nx vaccines but also for improving seasonal influenza vaccines and developing more effective broadly protective vaccines against other rapidly evolving RNA viruses.

Limitations of the study

We recognize that the comparison between DVX-panH5Nx (mRNA-LNP) and the CVV-derived WIV does not fully separate the effects of antigen design from those of vaccine platform. Platform-specific factors, such as antigen dose, expression kinetics, innate immune stimulation, formulation, and antigen presentation may contribute to the differences in immunogenicity observed. A more direct assessment would require a platform-matched comparator, such as an mRNA-LNP vaccine encoding the same HA-NA-M2 as the CVV strain in the WIV, which may be undertaken in future. Nonetheless, we have used the same DNA expression platform during our antigen-selection/comparison process, and although these data do not replace the platform-specific comparison, they support our premise of a broadly immunogenic antigen design that is not ascribed to the final mRNA-LNP formulation.

We also acknowledge that the dosing comparisons between the mRNA-LNP and the WIVs in the mouse studies may have influenced the magnitude and breadth of the immune response, including cross-reactivity against different H5 clades. We found it sufficient to employ a historical "protective" dose in mice of a single immunization of WIV[70] as benchmark for validating our initial DVX candidates. As part of a different study, we have done two WIV protein immunizations (Figure 4; Figures S4C–S4F), which show the immunogenicity of the 2-dose WIV; however, these responses were narrow and strain-specific compared to DVX candidates. Nonetheless, the main objective of the present study was to benchmark a next-generation vaccine against currently available countermeasures in ferrets, the gold standard animal model for human influenza to address the practical question facing preparedness programs: whether a broadly engineered pre-pandemic vaccine can provide greater protection than currently stockpiled CVV-based vaccines against contemporary and future H5Nx diversity.

RESOURCE AVAILABILITY

Lead contact

Requests for resources should be directed to and will be fulfilled by the lead contact, Jonathan L. Heeney (jlh66@cam.ac.uk).

Materials availability

Resources generated in this study will be made available on request, dependent on availability, and a completed materials transfer agreement if there is potential for commercial application.

Data and code availability

- The data supporting the results in this study are available within the paper and its supplemental information. Sequences used for designing vaccine antigens are from the publicly available GISAID database. Antigen sequences are patented under the international patent, WO2026074282,[48] and can be accessed at https://patentscope.wipo.int/search/en/detail.jsf?docId=WO2026074282&_cid=P12-MO19AU-33020-1.
- This paper does not include original code.
- Any additional information required to reanalyze the data reported in this paper is available from the lead contact upon request.

ACKNOWLEDGMENTS

We acknowledge all data contributors and submitting laboratories for generating and sharing genetic sequences and metadata via the GISAID Initiative on which this research is based. This work was in part funded by the UKRI under grant# UKRI/BB/D006475/1. We are thankful to etherna (Niel, Belgium) for the formulated mRNA; Dr. Francesco Gubinelli for the A/Astrakhan/3212/2020 (H5N8) antigen for our initial studies; Prof. Yoshihiro Kawaoka for the A/Vietnam/1203/2004 H5N1 challenge virus; the Department of Pathology, University of Cambridge, for sectioning and H&E staining of ferret tissues; and Prof. John McCauley, Dr. Othmar Engelhardt, and Dr. Jason Long for their pre-submission feedback on this manuscript.

AUTHOR CONTRIBUTIONS

Conceptualization, J.M.D, F.B., and J.L.H.; methodology, J.M.D, S.V., S.F., D.K., F.B., and J.L.H; software, S.V., S.F., and M.D.; validation, J.M.D., S.B.S., S.K.A., R.V., M.F., L.V., M.P., S.R., V.M.P., E.M., A.F., M.V., and T.T.; formal analysis, J.M.D., S.V., S.B.S., S.K.A., R.V., L.V., A.L.O., M.D., and F.B.; investigation, J.M.D., S.B.S., S.K.A., R.V., M.F., G.W.C., L.V., M.P., S.R., V.M.P., E.M., A.F., M.V., T.T., P.T., and M.S.; resources, B.A., N.J.T., and R.W.; data curation, S.V., S.F., S.K.A., and M.D.; visualization, S.V. and S.K.A.; supervision, J.M.D., B.A., R.W., D.K., F.B., and J.L.H.; project administration, J.M.D. and D.M.; funding acquisition, D.M.S., R.K., R.W., and J.L.H.; writing – original draft, J.M.D., S.V., S.B.S., D.M.S., F.B., and J.L.H.; writing – reviewing & editing, all authors.

DECLARATION OF INTERESTS

J.M.D., S.B.S., S.K.A., M.F., M.D., D.M., R.K., R.W., and J.L.H. are employees or shareholders of DIOSynVax Ltd. S.F. is an employee of Microsoft Research. The DVX antigen sequences have been patented under WO2026074282,[48] UK patent application no. GB2414517.8, influenza vaccines, PCT/GB2022/052534, and PCT/GB2024/052670 (influenza antigen synergies patent).

STAR★METHODS

Detailed methods are provided in the online version of this paper and include the following:

- KEY RESOURCES TABLE
- EXPERIMENTAL MODEL AND STUDY PARTICIPANT DETAILS
  - Ethics
  - Mice
  - Ferret
  - Cell lines
- METHOD DETAILS
  - In-silico design of vaccine antigens
  - DNA plasmids
  - mRNA-LNP vaccine candidates
  - Whole inactivated virus (WIV) antigens
  - Lentiviral pseudotype viruses
  - Influenza Viruses
  - Mouse immunogenicity studies
  - Mouse challenge studies
  - Ferret challenge study
  - Viral RNA quantification
  - Histopathology
  - Serological investigations
- QUANTIFICATION AND STATISTICAL ANALYSIS

SUPPLEMENTAL INFORMATION

Supplemental information can be found online at https://doi.org/10.1016/j.xcrm.2026.103131.

Received: February 25, 2026
Revised: July 26, 2026
Accepted: October 12, 2026

REFERENCES

1. Bird & mammal species affected by H5Nx HPAI (2026). Animal Health. https://www.fao.org/animal-health/situation-updates/global-aiv-with-zoonotic-potential/bird-species-affected-by-h5nx-hpai/en.
2. Graziosi, G., Lupini, C., Catelli, E., and Carnaccini, S. (2024). Highly Pathogenic Avian Influenza (HPAI) H5 Clade 2.3.4.4b Virus Infection in Birds and Mammals. Animals. *14*, 1372. https://doi.org/10.3390/ani14091372.
3. Mostafa, A., Naguib, M.M., Nogales, A., Barre, R.S., Stewart, J.P., García-Sastre, A., and Martinez-Sobrido, L. (2024). Avian influenza A (H5N1) virus in dairy cattle: origin, evolution, and cross-species transmission. mBio *15*, e02542-24. https://doi.org/10.1128/mbio.02542-24.
4. Leguia, M., Garcia-Glaessner, A., Muñoz-Saavedra, B., Juarez, D., Barrera, P., Calvo-Mac, C., Jara, J., Silva, W., Ploog, K., Amaro, L., et al. (2023). Highly pathogenic avian influenza A (H5N1) in marine mammals and seabirds in Peru. Nat. Commun. *14*, 5489. https://doi.org/10.1038/s41467-023-41182-0.
5. CDC (2026). H5 Bird Flu: Current Situation. Avian Influenza (Bird Flu). https://www.cdc.gov/bird-flu/situation-summary/index.html.
6. Ly, H. (2024). Highly pathogenic avian influenza H5N1 virus infection of companion animals. Virulence *15*, 2289780. https://doi.org/10.1080/21505594.2023.2289780.
7. Cumulative number of confirmed human cases for avian influenza A(H5N1) reported to WHO, 2003-2026, 8 May 2026 2026 https://www.who.int/publications/m/item/cumulative-number-of-confirmed-human-cases-for-avian-influenza-a(h5n1)-reported-to-who–2003-2026–8-may-2026.
8. Table: Human cases of H5N1 bird flu (2026). BNO News. https://bnonews.com/index.php/human-cases-of-h5n1-bird-flu/.
9. Siegers, J.Y., Xie, R., Edwards, K.M., Byrne, A.M.P., Hu, S., Wang, R., Yann, S., Sin, S., Tok, S., Chea, K., Horm, S., et al. (2025). Resurgence of Zoonotic Highly Pathogenic Avian Influenza A(H5N1) Virus in Cambodia. New England Journal of Medicine *393*, 1650–1652. https://doi.org/10.1056/NEJMc2504302.
10. Cambodia logs fourth fatal H5N1 avian flu case of the year | CIDRAP (2025). https://www.cidrap.umn.edu/avian-influenza-bird-flu/cambodia-logs-fourth-fatal-h5n1-avian-flu-case-year.
11. Sagulenko, P., Puller, V., and Neher, R.A. (2018). TreeTime: Maximum-likelihood phylodynamic analysis. Virus Evol. *4*, vex042. https://doi.org/10.1093/ve/vex042.
12. Hadfield, J., Megill, C., Bell, S.M., Huddleston, J., Potter, B., Callender, C., Sagulenko, P., Bedford, T., and Neher, R.A. (2018). Nextstrain: real-time tracking of pathogen evolution. Bioinformatics *34*, 4121–4123. https://doi.org/10.1093/bioinformatics/bty407.
13. Elbe, S., and Buckland-Merrett, G. (2017). Data, disease and diplomacy: GISAID's innovative contribution to global health. Glob. Chall. *1*, 33–46. https://doi.org/10.1002/gch2.1018.
14. Khare, S., Gurry, C., Freitas, L., Schultz, M.B., Bach, G., Diallo, A., Akite, N., Ho, J., Lee, R.T., Yeo, W., et al. (2021). GISAID's Role in Pandemic Response. China CDC Wkly. *3*, 1049–1051. https://doi.org/10.46234/ccdcw2021.255.
15. Shu, Y., and McCauley, J. (2017). GISAID: Global initiative on sharing all influenza data – from vision to reality. Euro Surveill. *22*, 30494. https://doi.org/10.2807/1560-7917.ES.2017.22.13.30494.
16. Strohmeier, S., Amanat, F., Zhu, X., McMahon, M., Deming, M.E., Pasetti, M.F., Neuzil, K.M., Wilson, I.A., and Krammer, F. (2021). A Novel Recombinant Influenza Virus Neuraminidase Vaccine Candidate Stabilized by a Measles Virus Phosphoprotein Tetramerization Domain Provides Robust Protection from Virus Challenge in the Mouse Model. mBio *12*, e02241-21. https://doi.org/10.1128/mBio.02241-21.
17. Yang, H., Carney, P.J., Mishin, V.P., Guo, Z., Chang, J.C., Wentworth, D.E., Gubareva, L.V., and Stevens, J. (2016). Molecular Characterizations of Surface Proteins Hemagglutinin and Neuraminidase from Recent H5Nx Avian Influenza Viruses. J. Virol. *90*, 5770–5784. https://doi.org/10.1128/jvi.00180-16.
18. European Centre for Disease Prevention and Control (2024). Zoonotic influenza. ECDC. Annual epidemiological report for 2024.
19. Rosu, M.E., Westgeest, K.B., De Graaf, M., Hauser, B.M., Tureli, S., James, S., Sinartio, F.F., Bestebroer, T.M., Lexmond, P., Pronk, M.R., et al. (2026). Molecular basis of 60 years of antigenic evolution of human influenza A(H3N2) virus neuraminidase. Cell Host Microbe *34*, 103–115.e9. https://doi.org/10.1016/j.chom.2025.12.006.

Please cite this article in press as: Del Rosario et al., Broad vaccine protection against globally diverse influenza A/H5Nx viruses, Cell Reports Medicine (2026), https://doi.org/10.1016/j.xcrm.2026.103131

20. He, M., Liu, L., Hu, J., Wang, Z., Guo, Z., Wang, X., Sun, Y., Shi, S., Ren, W., Wang, Y., et al. (2025). The H5N6 Virus Containing Internal Genes From H9N2 Exhibits Enhanced Pathogenicity and Transmissibility. Transbound. Emerg. Dis. *2025*, 6252849. https://doi.org/10.1155/tbed/6252849.

21. Bliss, C.M., Nachbagauer, R., Mariottini, C., Cuevas, F., Feser, J., Naficy, A., Bernstein, D.I., Guptill, J., Walter, E.B., Berlanda-Scorza, F., et al. (2024). A chimeric haemagglutinin-based universal influenza virus vaccine boosts human cellular immune responses directed towards the conserved haemagglutinin stalk domain and the viral nucleoprotein. EBioMedicine *104*, 105153. https://doi.org/10.1016/j.ebiom.2024.105153.

22. Sánchez-de Prada, L., Sanz-Muñoz, I., Sun, W., Palese, P., Ortiz de Lejarazu, R., Eiros, J.M., García-Sastre, A., and Aydillo, T. (2023). Group 1 and group 2 hemagglutinin stalk antibody response according to age. Front. Immunol. *14*, 1194073. https://doi.org/10.3389/fimmu.2023.1194073.

23. Zhang, L., Behrens, G.M.N., Kempf, A., Nehlmeier, I., Gärtner, S., Moldenhauer, A.-S., Graichen, L., Happle, C., Winkler, M., Dopfer-Jablonka, A., et al. (2025). Neutralizing activity against bovine H5N1 HPAIV (clade 2.3.4.4b) in human plasma after seasonal influenza vaccination. Emerg. Microbes Infect. *14*, 2528539. https://doi.org/10.1080/22221751.2025.2528539.

24. Restori, K.H., Weaver, V., Patel, D.R., Merrbach, G.A., Septer, K.M., Field, C.J., Bernabe, M.J., Kronthal, E.M., Minns, A., Lindner, S.E., et al. (2025). Preexisting immunity to the 2009 pandemic H1N1 virus reduces susceptibility to H5N1 infection and disease in ferrets. Sci. Transl. Med. *17*, eadw4856. https://doi.org/10.1126/scitranslmed.adw4856.

25. Sun, X., Subbiah, J., Belser, J.A., Brock, N., Gansebom, S., Li, Z.-N., Jung, Y.-J., Liu, F., Tumpey, T.M., Maines, T.R., et al. (2025). Effect of Seasonal Influenza Vaccines on Avian Influenza A(H5N1) Clade 2.3.4.4b Virus Infection in Ferrets. Emerg. Infect. Dis. *31*, 1950–1960. https://doi.org/10.3201/eid3110.250668.

26. Lv, K., Li, X., Zhu, X., Cai, J.-P., Liu, S., Sun, Y., Liu, L., Cai, X., Cao, R., Xu, M., et al. (2025). Broad neuraminidase antibodies confer protection against seasonal and avian influenza viruses. Nat. Commun. *16*, 7103. https://doi.org/10.1038/s41467-025-62040-1.

27. Job, E.R., Ysenbaert, T., Smet, A., Christopoulou, I., Strugnell, T., Oloo, E.O., Oomen, R.P., Kleanthous, H., Vogel, T.U., and Saelens, X. (2018). Broadened immunity against influenza by vaccination with computationally designed influenza virus N1 neuraminidase constructs. npj Vaccines *3*, 55. https://doi.org/10.1038/s41541-018-0093-1.

28. Skarlupka, A.L., Bebin-Blackwell, A.-G., Sumner, S.F., and Ross, T.M. (2021). Universal Influenza Virus Neuraminidase Vaccine Elicits Protective Immune Responses against Human Seasonal and Pre-pandemic Strains. J. Virol. *95*, e0075921. https://doi.org/10.1128/jvi.00759-21.

29. Singh, G., Bhavsar, D., Hermann, E., Gleason, C., Singh Sandhu, H., Singh, P., Nardulli, J.R., Lyttle, N., Chen, Y., Sabaiduc, S., et al. (2026). Population immunity to clade 2.3.4.4b H5N1 is dominated by anti-neuraminidase antibodies. mBio *17*, e00445-26. https://doi.org/10.1128/mbio.00445-26.

30. Signore, A.V., Joseph, T., Ranadheera, C., Erdelyan, C.N.G., Alkie, T.N., Raj, S., Pama, L., Ayilara, I., Hisanaga, T., Lung, O., et al. (2025). Neuraminidase reassortment and oseltamivir resistance in clade 2.3.4.4b A(H5N1) viruses circulating among Canadian poultry, 2024. Emerg. Microbes Infect. *14*, 2469643. https://doi.org/10.1080/22221751.2025.2469643.

31. Wolfe, M.K., Duong, D., Shelden, B., Chan, E.M.G., Chan-Herur, V., Hilton, S., Paulos, A.H., Xu, X.-R.S., Zulli, A., White, B.J., and Boehm, A.B. (2024). Detection of Hemagglutinin H5 Influenza A Virus Sequence in Municipal Wastewater Solids at Wastewater Treatment Plants with Increases in Influenza A in Spring, 2024. Environ. Sci. Technol. Lett. *11*, 526–532. https://doi.org/10.1021/acs.estlett.4c00331.

32. Peacock, T.P., Moncla, L., Dudas, G., VanInsberghe, D., Sukhova, K., Lloyd-Smith, J.O., Worobey, M., Lowen, A.C., and Nelson, M.I. (2025). The global H5N1 influenza panzootic in mammals. Nature *637*, 304–313. https://doi.org/10.1038/s41586-024-08054-z.

33. Paulos, A.P., Hilton, S.P., Shelden, B., Duong, D., Boehm, A.B., and Wolfe, M.K. (2025). Detection of Hemagglutinin H5 Influenza A Virus RNA and Model of Potential Inputs in an Urban California Sewershed. Environ. Sci. Technol. *59*, 16168–16179. https://doi.org/10.1021/acs.est.4c14792.

34. Gao, F., Wang, Q., Qiu, C., Luo, J., and Li, X. (2024). Pandemic preparedness of effective vaccines for the outbreak of newly H5N1 highly pathogenic avian influenza virus. Virol. Sin. *39*, 981–985. https://doi.org/10.1016/j.virs.2024.11.005.

35. Krammer, F., Fouchier, R.A.M., Eichelberger, M.C., Webby, R.J., Shaw-Saliba, K., Wan, H., Wilson, P.C., Compans, R.W., Skountzou, I., and Monto, A.S. (2018). NAction! How Can Neuraminidase-Based Immunity Contribute to Better Influenza Virus Vaccines? mBio *9*, e02332-17. https://doi.org/10.1128/mBio.02332-17.

36. Matsuoka, Y., Swayne, D.E., Thomas, C., Rameix-Welti, M.-A., Naffakh, N., Warnes, C., Altholtz, M., Donis, R., and Subbarao, K. (2009). Neuraminidase Stalk Length and Additional Glycosylation of the Hemagglutinin Influence the Virulence of Influenza H5N1 Viruses for Mice. J. Virol. *83*, 4704–4708. https://doi.org/10.1128/JVI.01987-08.

37. Li, F., Sun, Z., Tao, M., Song, K., Wang, Z., and Ren, X. (2024). Epidemiological characterization of human infection with H5N6 avian influenza. Front. Public Health *12*, 1398365. https://doi.org/10.3389/fpubh.2024.1398365.

38. Wang, L., and Gao, G.F. (2025). A brief history of human infections with H5Ny avian influenza viruses. Cell Host Microbe *33*, 176–181. https://doi.org/10.1016/j.chom.2025.01.010.

39. Zhou, L., Li, Z., Zhou, X., Zhao, L., Peng, H., Du, X., Yang, J., Hu, F., Dong, S., Li, B., et al. (2025). Investigation of human infection with H5N6 avian influenza cases in Sichuan Province from 2014 to 2024: a retrospective study. Front. Public Health *13*, 1603158. https://doi.org/10.3389/fpubh.2025.1603158.

40. Liang, Z., Lin, X., Sun, L., Edwards, K.M., Song, W., Sun, H., Xie, Y., Lin, F., Ling, S., Liang, T., et al. (2024). A(H2N2) and A(H3N2) influenza pandemics elicited durable cross-reactive and protective antibodies against avian N2 neuraminidases. Nat. Commun. *15*, 5593. https://doi.org/10.1038/s41467-024-49884-9.

41. Kok, A., Wilks, S.H., Tureli, S., James, S.L., Bestebroer, T.M., Burke, D.F., Funk, M., van der Vliet, S., Spronken, M.I., Rijnink, W.F., et al. (2025). A vaccine central in A(H5) influenza antigenic space confers broad immunity. Nature *647*, 1005–1013. https://doi.org/10.1038/s41586-025-09626-3.

42. Furey, C., Scher, G., Ye, N., Kercher, L., DeBeauchamp, J., Crumpton, J.C., Jeevan, T., Patton, C., Franks, J., Rubrum, A., et al. (2024). Development of a nucleoside-modified mRNA vaccine against clade 2.3.4.4b H5 highly pathogenic avian influenza virus. Nat. Commun. *15*, 4350. https://doi.org/10.1038/s41467-024-48555-z.

43. Hatta, M., Hatta, Y., Choi, A., Hossain, J., Feng, C., Keller, M.W., Ritter, J.M., Huang, Y., Fang, E., Pusch, E.A., et al. (2024). An influenza mRNA vaccine protects ferrets from lethal infection with highly pathogenic avian influenza A(H5N1) virus. Sci. Transl. Med. *16*, eads1273. https://doi.org/10.1126/scitranslmed.ads1273.

44. Sun, X., Belser, J.A., Pulit-Penaloza, J.A., Creager, H.M., Guo, Z., Jefferson, S.N., Liu, F., York, I.A., Stevens, J., Maines, T.R., et al. (2017). Stockpiled pre-pandemic H5N1 influenza virus vaccines with AS03 adjuvant provide cross-protection from H5N2 clade 2.3.4.4 virus challenge in ferrets. Virology *508*, 164–169. https://doi.org/10.1016/j.virol.2017.05.010.

45. Sun, W., Xu, J., Wang, Z., Li, D., Sun, Y., Zhu, M., Liu, X., Li, Y., Li, F., Wang, T., et al. (2023). Clade 2.3.4.4 H5 chimeric cold-adapted attenuated influenza vaccines induced cross-reactive protection in mice and ferrets. J. Virol. *97*, e01101-23. https://doi.org/10.1128/jvi.01101-23.

46. Khurana, S., King, L.R., Manischewitz, J., Posadas, O., Mishra, A.K., Liu, D., Beigel, J.H., Rappuoli, R., Tsang, J.S., and Golding, H. (2024). Licensed H5N1 vaccines generate cross-neutralizing antibodies against highly pathogenic H5N1 clade 2.3.4.4b influenza virus. Nat. Med. *30*, 2771–2776. https://doi.org/10.1038/s41591-024-03189-y.

47. Vishwanath, S., Carnell, G.W., Ferrari, M., Asbach, B., Billmeier, M., George, C., Sans, M.S., Nadesalingam, A., Huang, C.Q., Paloniemi, M., et al. (2025). A computationally designed antigen eliciting broad humoral responses against SARS-CoV-2 and related sarbecoviruses. Nat. Biomed. Eng. *9*, 153–166. https://doi.org/10.1038/s41551-023-01094-2.

48. Vishwanath, S., Carnell, G., Del Rosario, J., and Heeney, J. (2026). Influenza Vaccines. https://patentscope.wipo.int/search/en/detail.jsf?docId=WO2026074282&_cid=P12-MO19AU-33020-1.

49. NCBI Virus (2026). https://www.ncbi.nlm.nih.gov/labs/virus/vssi/#/.

50. Del Rosario, J.M.M., Da Costa, K.A.S., Asbach, B., Ferrara, F., Ferrari, M., Wells, D.A., Mann, G.S., Ameh, V.O., Sabeta, C.T., Banyard, A.C., et al. (2021). Exploiting Pan Influenza A and Pan Influenza B Pseudotype Libraries for Efficient Vaccine Antigen Selection. Vaccines *9*, 741. https://doi.org/10.3390/vaccines9070741.

51. Carnell, G.W., Trombetta, C.M., Ferrara, F., Montomoli, E., and Temperton, N.J. (2021). Correlation of Influenza B Haemagglutination Inhibiton, Single-Radial Haemolysis and Pseudotype-Based Microneutralisation Assays for Immunogenicity Testing of Seasonal Vaccines. Vaccines (Basel) *9*, 100. https://doi.org/10.3390/vaccines9020100.

52. Carnell, G.W., Ciazynska, K.A., Wells, D.A., Xiong, X., Aguinam, E.T., McLaughlin, S.H., Mallery, D., Ebrahimi, S., Ceron-Gutierrez, L., Asbach, B., et al. (2021). SARS-CoV-2 Spike Protein Stabilized in the Closed State Induces Potent Neutralizing Responses. J. Virol. *95*, e0020321. https://doi.org/10.1128/jvi.00203-21.

53. Da Costa, K.A.S., Del Rosario, J.M.M., Ferrari, M., Vishwanath, S., Asbach, B., Kinsley, R., Wagner, R., Heeney, J.L., Carnell, G.W., and Temperton, N.J. (2022). Influenza A (N1-N9) and Influenza B (B/Victoria and B/Yamagata) Neuraminidase Pseudotypes as Tools for Pandemic Preparedness and Improved Influenza Vaccine Design. Vaccines *10*, 1520. https://doi.org/10.3390/vaccines10091520.

54. Pardi, N., Hogan, M.J., Porter, F.W., and Weissman, D. (2018). mRNA vaccines — a new era in vaccinology. Nat. Rev. Drug Discov. *17*, 261–279. https://doi.org/10.1038/nrd.2017.243.

55. Wang, C., and Yuan, F. (2024). A comprehensive comparison of DNA and RNA vaccines. Adv. Drug Deliv. Rev. *210*, 115340. https://doi.org/10.1016/j.addr.2024.115340.

56. De Lombaerde, E., Chen, Y., Ye, T., Deckers, J., Mencarelli, G., De Swarte, K., Lauwers, H., De Coen, R., Kasmi, S., Bevers, S., et al. (2024). Combinatorial Screening of Biscarbamate Ionizable Lipids Identifies a Low Reactogenicity Lipid for Lipid Nanoparticle mRNA Delivery. Adv. Funct. Mater. *34*, 2310623. https://doi.org/10.1002/adfm.202310623.

57. De Coen, R., Kasmi, S., Dumbre, S., Baekens, L., Seynaeve, E., Van Den Hauwe, L., Cantini, N., Garantoudi, A., Madeira, F.B., Marrot, A., et al. (2025). Next-Generation Bio-Reducible Lipids Enable Enhanced Vaccine Efficacy in Malaria and Primate Models. Adv. Funct. Mater. *36*, e09838. https://doi.org/10.1002/adfm.202509838.

58. Cagigi, A., and Douradinha, B. (2023). Have mRNA vaccines sentenced DNA vaccines to death? Expert Rev. Vaccines *22*, 1154–1167. https://doi.org/10.1080/14760584.2023.2282065.

59. Szymczak-Workman, A.L., Vignali, K.M., and Vignali, D.A.A. (2012). Design and construction of 2A peptide-linked multicistronic vectors. Cold Spring Harb. Protoc. *2012*, 199–204. https://doi.org/10.1101/pdb.ip067876.

60. Caserta, L.C., Frye, E.A., Butt, S.L., Laverack, M., Nooruzzaman, M., Covaleda, L.M., Thompson, A.C., Koscielny, M.P., Cronk, B., Johnson, A., et al. (2024). Spillover of highly pathogenic avian influenza H5N1 virus to dairy cattle. Nature *634*, 669–676. https://doi.org/10.1038/s41586-024-07849-4.

61. Jassem, A.N., Roberts, A., Tyson, J., Zlosnik, J.E.A., Russell, S.L., Caleta, J.M., Eckbo, E.J., Gao, R., Chestley, T., Grant, J., et al. (2025). Critical Illness in an Adolescent with Influenza A(H5N1) Virus Infection. N. Engl. J. Med. *392*, 927–929. https://doi.org/10.1056/NEJMc2415890.

62. Tsybalova, L.M., Stepanova, L.A., Kuprianov, V.V., Blokhina, E.A., Potapchuk, M.V., Korotkov, A.V., Gorshkov, A.N., Kasyanenko, M.A., Ravin, N.V., and Kiselev, O.I. (2015). Development of a candidate influenza vaccine based on virus-like particles displaying influenza M2e peptide into the immunodominant region of hepatitis B core antigen: Broad protective efficacy of particles carrying four copies of M2e. Vaccine *33*, 3398–3406. https://doi.org/10.1016/j.vaccine.2015.04.073.

63. Kavishna, R., Kang, T.Y., Vacca, M., Chua, B.Y.L., Park, H.-Y., Tan, P.S., Chow, V.T., Lahoud, M.H., and Alonso, S. (2022). A single-shot vaccine approach for the universal influenza A vaccine candidate M2e. Proc. Natl. Acad. Sci. USA *119*, e2025607119. https://doi.org/10.1073/pnas.2025607119.

64. Neirynck, S., Deroo, T., Saelens, X., Vanlandschoot, P., Jou, W.M., and Fiers, W. (1999). A universal influenza A vaccine based on the extracellular domain of the M2 protein. Nat. Med. *5*, 1157–1163. https://doi.org/10.1038/13484.

65. Sakala, I.G., Honda-Okubo, Y., Li, L., Baldwin, J., and Petrovsky, N. (2021). A M2 protein-based universal influenza vaccine containing Advax-SM adjuvant provides newborn protection via maternal or neonatal immunization. Vaccine *39*, 5162–5172. https://doi.org/10.1016/j.vaccine.2021.07.037.

66. Belser, J.A., Katz, J.M., and Tumpey, T.M. (2011). The ferret as a model organism to study influenza A virus infection. Dis. Model. Mech. *4*, 575–579. https://doi.org/10.1242/dmm.007823.

67. Rioux, M., Francis, M.E., Swan, C.L., Ge, A., Kroeker, A., and Kelvin, A.A. (2021). The Intersection of Age and Influenza Severity: Utility of Ferrets for Dissecting the Age-Dependent Immune Responses and Relevance to Age-Specific Vaccine Development. Viruses *13*, 678. https://doi.org/10.3390/v13040678.

68. Hatta, Y., Hill-Batorski, L., Moser, M.J., Marshall, D., Boltz, D.A., Westfall, L., Herber, R., Sarawar, S., and Bilsel, P. (2024). Intranasal M2SR and BM2SR Vaccine Viruses Do Not Shed or Transmit in Ferrets. Vaccines (Basel) *12*, 1228. https://doi.org/10.3390/vaccines12111228.

69. Uno, N., and Ross, T.M. (2024). Multivalent next generation influenza virus vaccines protect against seasonal and pre-pandemic viruses. Sci. Rep. *14*, 1440. https://doi.org/10.1038/s41598-023-51024-0.

70. Del Rosario, J.M.M. (2020). Immunoprophylaxis of Influenza Using AAV Vector Delivery of Cross-Subtype Neutralizing Nanobodies [PhD Thesis] (University College London). https://discovery.ucl.ac.uk/id/eprint/10107208/.

71. Dreyfus, C., Laursen, N.S., Kwaks, T., Zuijdgeest, D., Khayat, R., Ekiert, D.C., Lee, J.H., Metlagel, Z., Bujny, M.V., Jongeneelen, M., et al. (2012). Highly Conserved Protective Epitopes on Influenza B Viruses. Science *337*, 1343–1348. https://doi.org/10.1126/science.1222908.

72. Corti, D., Voss, J., Gamblin, S.J., Codoni, G., Macagno, A., Jarrossay, D., Vachieri, S.G., Pinna, D., Minola, A., Vanzetta, F., et al. (2011). A Neutralizing Antibody Selected from Plasma Cells That Binds to Group 1 and Group 2 Influenza A Hemagglutinins. Science *333*, 850–856. https://doi.org/10.1126/science.1205669.

73. Nguyen, L.-T., Schmidt, H.A., von Haeseler, A., and Minh, B.Q. (2015). IQ-TREE: A Fast and Effective Stochastic Algorithm for Estimating Maximum-Likelihood Phylogenies. Mol. Biol. Evol. *32*, 268–274. https://doi.org/10.1093/molbev/msu300.

74. Pond, S.L.K., Frost, S.D.W., and Muse, S.V. (2005). HyPhy: hypothesis testing using phylogenies. Bioinformatics *21*, 676–679. https://doi.org/10.1093/bioinformatics/bti079.

75. Katoh, K., Misawa, K., Kuma, K.i., and Miyata, T. (2002). MAFFT: a novel method for rapid multiple sequence alignment based on fast Fourier transform. Nucleic Acids Res. *30*, 3059–3066. https://doi.org/10.1093/nar/gkf436.

76. Percie du Sert, N., Hurst, V., Ahluwalia, A., Alam, S., Avey, M.T., Baker, M., Browne, W.J., Clark, A., Cuthill, I.C., Dirnagl, U., et al. (2020). The ARRIVE guidelines 2.0: Updated guidelines for reporting animal research. PLoS Biol. *18*, e3000410. https://doi.org/10.1371/journal.pbio.3000410.

Please cite this article in press as: Del Rosario et al., Broad vaccine protection against globally diverse influenza A/H5Nx viruses, Cell Reports Medicine (2026), https://doi.org/10.1016/j.xcrm.2026.103131

77. Neumann, G., Watanabe, T., Ito, H., Watanabe, S., Goto, H., Gao, P., Hughes, M., Perez, D.R., Donis, R., Hoffmann, E., et al. (1999). Generation of influenza A viruses entirely from cloned cDNAs. Proc. Natl. Acad. Sci. USA *96*, 9345–9350. https://doi.org/10.1073/pnas.96.16.9345.

78. Reed, L.J., and Muench, H. (1938). A Simple Method Of Estimating Fifty Per Cent Endpoints. Am. J. Epidemiol. *27*, 493–497. https://doi.org/10.1093/oxfordjournals.aje.a118408.

79. Wong, S.-S., Duan, S., DeBeauchamp, J., Zanin, M., Kercher, L., Sonnberg, S., Fabrizio, T., Jeevan, T., Crumpton, J.-C., Oshansky, C., et al. (2017). The immune correlates of protection for an avian influenza H5N1 vaccine in the ferret model using oil-in-water adjuvants. Sci. Rep. *7*, 44727. https://doi.org/10.1038/srep44727.

80. Leroux-Roels, I., Borkowski, A., Vanwolleghem, T., Dramé, M., Clement, F., Hons, E., Devaster, J.-M., and Leroux-Roels, G. (2007). Antigen sparing and cross-reactive immunity with an adjuvanted rH5N1 prototype pandemic influenza vaccine: a randomised controlled trial. Lancet *370*, 580–589. https://doi.org/10.1016/S0140-6736(07)61297-5.

81. Baras, B., Stittelaar, K.J., Simon, J.H., Thoolen, R.J.M.M., Mossman, S.P., Pistoor, F.H.M., van Amerongen, G., Wettendorff, M.A., Hanon, E., and Osterhaus, A.D.M.E. (2008). Cross-Protection against Lethal H5N1 Challenge in Ferrets with an Adjuvanted Pandemic Influenza Vaccine. PLoS One *3*, e1401. https://doi.org/10.1371/journal.pone.0001401.

82. Nagy, C., Maitra, M., Tanti, A., Suderman, M., Théroux, J.-F., Davoli, M.A., Perlman, K., Yerko, V., Wang, Y.C., Tripathy, S.J., et al. (2020). Single-nucleus transcriptomics of the prefrontal cortex in major depressive disorder implicates oligodendrocyte precursor cells and excitatory neurons. Nat. Neurosci. *23*, 771–781. https://doi.org/10.1038/s41593-020-0621-y.

83. Del Rosario, J.M.M., da Costa, K.A.S., and Temperton, N. (2023). Pseudotyped Viruses for Influenza. In Pseudotyped Viruses (Springer), pp. 153–173. https://doi.org/10.1007/978-981-99-0113-5_8.

84. (2021). Avian Influenza (Including Infection with High Pathogenicity Avian Influenza Viruses). In World Organisation for Animal Health Terrestrial Manual 2021World Organisation for Animal Health Terrestrial Manual 2021.

85. Oftung, F., Næss, L.M., Laake, I., Stoloff, G., and Pleguezuelos, O. (2022). FLU-v, a Broad-Spectrum Influenza Vaccine, Induces Cross-Reactive Cellular Immune Responses in Humans Measured by Dual IFN-γ and Granzyme B ELISpot Assay. Vaccines *10*, 1528. https://doi.org/10.3390/vaccines10091528.

Please cite this article in press as: Del Rosario et al., Broad vaccine protection against globally diverse influenza A/H5Nx viruses, Cell Reports Medicine (2026), https://doi.org/10.1016/j.xcrm.2026.103131

STAR★METHODS

KEY RESOURCES TABLE

REAGENT or RESOURCE	SOURCE	IDENTIFIER
Antibodies		
Mouse anti-Influenza A Antibody, nucleoprotein, Primary antibody	Merck Millipore	Cat#MAB8257; RRID: AB_95231; Cat#MAB8258; RRID: AB_95232
Peroxidase AffiniPure® Goat Anti-Mouse IgG (H + L) - Secondary Antibody	Jackson ImmunoResearch	Cat#115–035–003; RRID: AB_10015289
Anti-ferret IFN-γ mAb (MTF19), biotin-Detection antibody	Mabtech	Cat#MTF19
Phycoerythrin labeled anti-mouse Goat Anti-Mouse IgG H&L (PE)	Abcam	Cat#ab97024; RRID: AB_10698222
Goat anti-Ferret IgG (H + L) Secondary Antibody (PE)	Novus Biologicals	Cat#NB7222PE; RRID:AB_2895318
Goat Anti-Ferret IgG H&L (HRP) - Secondary antibody	Abcam	Cat#AB112770; RRID: AB_10862402
13D4, Anti-Hemagglutinin (A/Vietnam/1194/2004 H5N1) antibody	ABCD antibodies	Cat#ABCD_AI829
FLD21.140 HA, Anti-Hemagglutinin (A/Hong Kong/212/2003 H5N1) antibody	ABCD antibodies	Cat#ABCD_AI813
CR9114	Produced in-house; Dreyfus et al.[71]	RRID: AB_3752563
FI6	Produced in-house; Corti et al.[72]	N/A
Bacterial and virus strains		
DH5-α *E. coli* cells	Invitrogen	Cat#EC0112
A/chicken/Italy/23VIR3799-1/2023 (H5N1), GISAID ID: EPI_ISL_19767156	This paper	N/A
A/British Columbia/PHL-2032/2024 (H5N1), GISAID ID: EPI_ISL_19548836	This paper	N/A
A/Cambodia/NPH230032/2023 (H5N1), GISAID ID: GISAID EPI_ISL_17024123	This paper	N/A
A/Vietnam/1203/2004 (H5N1)	Kindly provided by Yoshihiro Kawaoka, University of Wisconsin-Madison	N/A
A/Astrakhan/3212/2020 (H5N8)	NIBSC; CDC	Cat#23/178, CBER-RG8A; IDCDC-RG71A
A/Vietnam/1194/2004 (H5N1)	NIBSC	Cat#09/184, NIBRG-14
A/turkey/Turkey/2005 (H5N1)	NIBSC	Cat#07/112, NIBRG-23
A/duck/Bangladesh/17D1012/2018 (H5N1)	CDC	IDCDC-RG63A
A/duck/Vietnam/NCVD-1584/2012 (H5N1)	NIBSC	Cat#17/142, NIBRG-301
A/Anhui/1/2005 (H5N1)	CDC	IBCDC-RG6
A/gyrfalcon/Washington/41088–6/2014 (H5N8)	CDC	IDCDC-RG43A
Biological samples		
Chicken Blood Cells (Adult) in Alsever's	TCS biosciences	Cat#FB013AP
Turkey Red Blood cells Packed 5%	Stratech Bioscience	Cat#ITKRBC5P-MIN
Chemicals, peptides, and recombinant proteins		
Paraformaldehyde	Thermo Scientific	Cat#J61899.AK; CAS: 30525–89–4
TrueBlue™ peroxidase substrate	SeraCare	Cat#A9647
Bright-Glo™ luciferase assay substrate	Promega	Cat#E2620
Fetuin	Sigma	Cat#F3385; CAS: 9014–81–7

(*Continued on next page*)

Please cite this article in press as: Del Rosario et al., Broad vaccine protection against globally diverse influenza A/H5Nx viruses, Cell Reports Medicine (2026), https://doi.org/10.1016/j.xcrm.2026.103131

Continued

REAGENT or RESOURCE	SOURCE	IDENTIFIER
Bovine serum albumin	Sigma, Sigma	Cat#A2153; Cat#A1470; CAS: 9048–46–8
1-Step™ Ultra TMB-ELISA Substrate Solution	Thermo Scientific	Cat#34029 CAS: 54827–17–7
Recombinant Influenza A H5N1 M2 protein from A/chicken/Hebei/326/2005 (H5N1)	Stratech	Cat#LS-G56682-LSP
Adipic acid dihydrazide	Sigma	Cat#A0638; CAS: 1071–93–8
Critical commercial assays		
QIAprep® Spin Miniprep Kit	Qiagen	Cat#27106
EndoFree® Plasmid Mega Kit	Qiagen	Cat#12381
MagMax CORE Nucleic Acid Purification Kit	Thermo Scientific	Cat#A32700
QIAcuity OneStep Advanced Probe Kit	Qiagen	Cat#250131
Ferret IFN-γ ELISpot Plus Kit	Mabtech	Cat#3112-4APW-2
ID Screen Influenza H5 Antibody Competition 3.0 Multi-Species ELISA Kit	IDVet	Cat#FLUACH5V3 ver 0724 EN
ID Screen Influenza H5 Indirect ELISA Kit	IDVet	Cat#FLUH5S ver 1221 EN
Deposited data		
DVX antigen sequences	This paper; Vishwanath et al.[48]	https://patentscope.wipo.int/search/en/detail.jsf?docId=WO2026074282&_cid=P12-MO19AU-33020-1
Experimental models: Cell lines		
Human Embryonic Kidney cells (HEK293T/17)	ATCC	ATCC-CRL-11268
Madin-Darby Canine Kidney cells (MDCK)	ATCC	ATCC-CCL-34
Experimental models: Organisms/strains		
Mouse: 028BALB/C Female BALB/C	Charles River UK; Charles River, Canada	RRID:IMSR_CRL:028
Ferret: *Mustela putorius furo*	BUSBUS-Euroferret	N/A
Recombinant DNA		
Influenza wildtype codon optimised HA, NA and M2 in pEVAC vector	This paper; GeneArt, Thermo Scientific	N/A
Influenza wildtype codon optimised HA in pI.18 vector	Del Rosario et al.[50]	N/A
Luciferase reporter plasmid (pCSFLW)	Del Rosario et al.[50]	N/A
Lentiviral packaging plasmid expressing gag and pol (p8.91)	Del Rosario et al.[50]	N/A
Transmembrane serine protease plasmid (TMPRSS4)	Del Rosario et al.[50]	N/A
Software and algorithms		
IQ-tree algorithm	Nguyen et al.[73]	https://doi.org/10.1093/molbev/msu300
PyMOL Molecular Graphics System, Version 3.0 Schrödinger, LLC	The PyMOL Molecular Graphics System, Version 3.0 Schrödinger, LLC.	https://www.pymol.org/
HyPhy	Pond et al.[74]	https://doi.org/10.1093/bioinformatics/bti079
MAFFT	Katoh et al.[75]	https://doi.org/10.1093/nar/gkf436
R studio	Posit Software, PBC	https://docs.posit.co/ide/user/#rstudio-ide-oss-downloads
QIAcuity Software Suite v. 2.5.0.1	Qiagen	N/A
GraphPad Prism v. 10.4.1	GraphPad	https://www.graphpad.com/
Other		
Fetal bovine serum	Thermo Scientific; Sial	A5256801; yourSIAL-FBS-SA

(*Continued on next page*)

Please cite this article in press as: Del Rosario et al., Broad vaccine protection against globally diverse influenza A/H5Nx viruses, Cell Reports Medicine (2026), https://doi.org/10.1016/j.xcrm.2026.103131

Continued

REAGENT or RESOURCE	SOURCE	IDENTIFIER
Penicillin/Streptomycin	Thermo Scientific, Euroclone	15140–122, ECB3001D
Dulbecco's Phosphate Buffer Saline (DPBS) no calcium, no magnesium	Thermo Scientific	Cat#10010031
DPBS, calcium, Magnesium	Thermo Scientific	Cat#14040091
PBS tablets	Thermo Scientific	Cat#18912014
Lectin from *Arachis hypogea* (peanut) peroxidase conjugate	Sigma	Cat#L7759
Recepter-destroying enzyme- II	Deben Diagnostics Ltd.	Cat#370013
FuGENE® HD	Promega	Cat#E231A
Exogenous neuraminidase	Merck	Cat#N2876
Addavax MF59 adjuvant	InvivoGen	Cat#vac-adx-10
Dulbecco's Modified Eagle Medium	Thermo Scientific; Gibco	Cat#31966021; Cat#41695–039
Opti-MEM	Thermo Scientific	Cat#31985070
Minimum Essential Medium	Sigma	Cat#M0275
Seaplaque® agarose	Lonza	Cat#50101
Bead Ruptor Elite Tissue Homogeniser	Omni	https://www.fishersci.co.uk/shop/products/bead-ruptor-elite-bead-mill-homogenizer/18839514
KingFisher Flex	Thermo Scientific	https://www.thermofisher.com/order/catalog/product/5400610
Myra Liquid Handling System	Bio Molecular Systems	Cat#MYRA-LHS50
QIAcuity Digital PCR System	Qiagen	Cat#911035
GloMax® Navigator	Promega	Cat#GM2000
Microplate reader	Agilent	Cat#BioTek 800 TS
CTL-Immunospot S6 Ultra Analyzer	Immunospot	https://immunospot.com/immunospot-s6-ultra-m2.html
Bio-Plex Pro™ magnetic COOH beads	Bio-Rad	MC1-0014-01 and MC1-0100-01
Bio-Plex® Handheld Magnetic Washer	Bio-Rad	Cat#171020100
Blocking solution	Candor-bioscience	Cat#110125
Bio-Plex 200 System	Bio-Rad	Cat#171000201
SureSense™ scanner	MSD Animal Health	Cat#HRPG1N
HEPA-filtered isolator	Montair	Cat#HM 1900

EXPERIMENTAL MODEL AND STUDY PARTICIPANT DETAILS

Ethics

Mouse immunogenicity studies were approved by the Animal Welfare Ethical Review Body (AWERB), University of Cambridge (Project license PP9157246). Studies were conducted per UK Home Office regulations under the Animals (Scientific Procedures) Act 1986 (ASPA) and results are reported according to the ARRIVE Guidelines.[76]

Mouse challenge studies were conducted as outlined in the Animal Use Document Application H-23–004, "Evaluation of vaccine candidates against HPAI H5N1 influenza". This was approved by the Canadian Science Center for Human & Animal Health - Animal Care Committee (CSCHAH - ACC) in accordance with the Canadian Council on Animal Care (CCAC).

Animal experimental procedures in ferrets were conducted in strict accordance with the Decree of the Italian Ministry of Health n. 26 of 4 March 2014 on the protection of animals used for scientific purposes, implementing Directive 2010/63/EU, and approved by the Institute's Ethic Committee (protocol n. 4/19 obtained on 15/1/2020). Animal experiments were approved by the Ministry of Health (709/2020-PR, further amended by 5351–24/02/2025-DGSAF-MDS-P).

Mice

For all mouse immunogenicity studies, 6–8 week-old female BALB/c mice were obtained from Charles River Laboratories and housed in separate groups of 6 mice each at the University Biomedical Services, University of Cambridge.

For mice challenge studies, six week old BALB/c mice (Charles River, Canada), equally divided between males and females, were allocated at Biosafety level 2 (BSL2) in the animal facility of the National Microbiology Laboratory in Winnipeg (NML), MB (Public Health Agency of Canada).

Ferret

Type A Influenza antibody-free male ferrets (*Mustela putorius furo*), 16 weeks of age, were purchased from BUSBUS-Euroferret, allocated in the BSL2 animal facilities of the Istituto Zooprofilattico Sperimentale delle Venezie (IZSVe), Legnaro, Italy, and identified with subcutaneous implantation of the Mini Thermochip sensors (MSD Animal Health, UIN 386923).

Cell lines

Human Embryonic Kidney cells (HEK293T/17) (ATCC-CRL-11268) and Madin-Darby Canine Kidney cells (MDCK) (ATCC-CCL-34) were obtained from American Type Culture collection (ATCC). HEK293T/17 cells were propagated and maintained in complete Dulbecco's Modified Essential medium (1X DMEM-GlutaMax (Thermo Scientific, 31966021) supplemented with 10% (v/v) Fetal Bovine Serum (FBS) (Thermo Scientific, A5256801, heat inactivated at 56°C) and 1% (v/v) Penicillin/Streptomycin (Thermo Scientific, 15140–122)) at 37°C, 5% CO_2.

MDCK cells were maintained at 37°C in a 5% CO_2 incubator in DMEM (Gibco, 41695–039) supplemented with 10% FBS (Sial, yourSIAL-FBS-SA), 1% of a 2:3 (v/v) penicillin-streptomycin solution (10,000 Unit/mL) (Euroclone-ECB3001D) and a 1:3 (v/v) nystatin solution (Sigma, N1638) (10,000 Unit/ml) in Dulbecco's phosphate-buffered saline (DPBS) (Sigma, D8537).

The HEK293T/17 and MDCK cells both tested negative for mycoplasma contamination via a commercial kit MycoStrip (Invivogen, rep-mys-10). Both cell lines have not been authenticated.

METHOD DETAILS

In-silico design of vaccine antigens

The nucleotide sequences of hemagglutinin (HA), neuraminidase (NA), and matrix protein (M2) of H5Nx subtype were obtained from the GISAID[13–15] and NCBI[49] databases. The sequence datasets were utilised to generate unique antigen sequences for HA, NA, and M2 which are phylogenetically closest to all the input sequences in comparison to any sequence in the downloaded dataset. The DVX-H5-1, DVX-N1, DVX-N6, and DVX-M2 designs were generated using sequences submitted up to April 2019, and DVX-H5-2 was generated using sequences submitted up to December 2020. In brief, for HA, NA, and M2, the sequences were trimmed to the coding regions and filtered for redundancy at 95% sequence identity using the MAFFT[75] algorithm. Multiple sequence alignment (MSA) of HA, NA, and M2 was generated with default parameters. Phylogenetic trees for HA, NA, and M2 were produced using the previously generated MSA using IQ-tree algorithm.[73] The optimal nucleotide model for phylogenetic tree generation was chosen according to Bayesian information criteria (BIC) score. The phylogenetic tree and MSA were used as input to Hyphy[74] to generate antigens.

DNA plasmids

For selection of immune-optimised antigens *in vivo*, DVX-H5-1, DVX-H5-2, DVX-N1, DVX-N6, DVX-M2, and wild-type hemagglutinin (H5), neuraminidase (N1, N6), and M2 antigens as controls (Table S2A), were cloned in pEVAC plasmids (GeneArt). Additionally, wild type H5, N1, and N6 were also cloned in pEVAC or pI.18 plasmids to produce DNA for transfections to make lentiviral pseudotyped viruses (Tables S3A and S3B) for pMN and pELLA. Plasmids were transformed via heat-shock into competent DH5-α *E. coli* (Invitrogen, EC0112) cells. DNA was extracted from bacterial cultures using the Qiagen plasmid DNA extraction kit (QIAprep Spin Miniprep Kit, 27106) for pseudotype production, and via the EndoFree Plasmid Mega Kit (QIAGEN, 12381) for production of DNA for immunogenicity studies. Plasmid DNA was then quantified using UV spectrophotometry (Nanodrop 1000, ThermoFisher, UK) and a sequence integrity check was done by Sanger sequencing (Source Bioscience, UK).

mRNA-LNP vaccine candidates

The DVX antigens were made into mRNA in Lipid Nano Particles (LNP) by etherna (Niel, Belgium). Briefly, the mRNA vaccine candidates were transcribed *in vitro* from a linearised plasmid DNA template encoding 5′ and 3′ untranslated regions and a polyadenosine tail. Co-transcriptional capping was performed using CleanCap AG (Trilink). The LNPs were formulated using the S-Ac7-DOG ionisable lipid.[56]

Whole inactivated virus (WIV) antigens

All WIV vaccines (Tables S2B–S2D) were purchased from the National Institutes of Biological Standards and Control (NIBSC), Medicines and Healthcare Products Regulatory Agency (MHRA) of the United Kingdom and have been inactivated following validated procedures used to produce human influenza vaccine that is registered in the EU. These inactivated reagent standards have been shown to be free from residual infectious virus by testing according to the European Pharmacopeia Compendial Assay (monograph 0158). The doses refer to hemagglutinin content and not total protein.

Please cite this article in press as: Del Rosario et al., Broad vaccine protection against globally diverse influenza A/H5Nx viruses, Cell Reports Medicine (2026), https://doi.org/10.1016/j.xcrm.2026.103131

Lentiviral pseudotype viruses

HEK293T/17 (4.1×10^5 cells per well) were seeded in 6-well tissue culture plates (Griener Bio-one, 657160) in complete DMEM. Next day, media in the plates was replaced and a transfection mix was prepared by combining the following plasmids in 100 μL Opti-MEM (Thermo Scientific, 31985070) with FuGENE HD (Promega, E231A) at 3 μL per μg of DNA: 10–50 ng pEVAC or pI.18 plasmids encoding for HA or NA genes, 250 ng p8.91 plasmid (gag pol), 375 ng Luciferase reporter plasmid (pCSFLW). For NA pseudotype viruses, additional 10 ng H11 gene encoding plasmid (A/red shoveler/Chile/C14653/2016) and 10 ng transmembrane serine protease plasmid (TMPRSS4) were also employed. The transfection mix was incubated for 15 min at room temperature. After incubation, cells were transfected with 100 μL of transfection mix per well and incubated at 37°C, 5% CO_2 for 72 h. For HA plasmids, 1 unit per well of exogenous neuraminidase (Merck, N2876) was added 14–16 h post transfection. The pseudotype viruses were harvested by collecting the supernatant. Supernatant was filtered using a 0.45 μm Millex MCE syringe filter (Merck Millipore, SLHAR33SB) and stored at −80°C.

Influenza Viruses

For the mouse challenge study, the following three HPAI H5N1 viruses were selected: i) A/British Columbia/PHL-2032/2024 (clade 2.3.4.4b; GISAID EPI_ISL_19548836), ii) A/Cambodia/NPH230032/2023 (clade 2.3.2.1.e; GISAID EPI_ISL_17024123), and iii) A/Vietnam/1203/2004 (clade 1; ABP51977.1). A/British Columbia/PHL-2032/2024 was isolated by passage of a tracheal aspirate sample on MDCK cells and passaged twice on MDCK to generate a P3 stock. A/Cambodia/NPH230032/2023 (KHM/2023 HN), a recombinant virus containing the HA and NA of A/Cambodia/NPH230032/2023 in a background of other genes derived from A/Astrakhan/3212/2020, was generated by reverse genetics[77] and was passaged on MDCK cells. A/Vietnam/1203/2004, was kindly provided by Yoshihiro Kawaoka, University of Wisconsin-Madison, and passaged on MDCK cells. All viruses were titrated by standard plaque assay on MDCK cells using Minimal Essential Medium (MEM) (Sigma, M0275),1% Seaplaque agarose (Lonza, 50101) overlay containing 0.75 μg/mL TPCK-trypsin (Sigma, T1426) and 0.1% Bovine Serum Albumin (BSA) (Sigma, A1470).The HPAI H5N1 A/chicken/Italy/23VIR3799-1/2023 (EPI_ISL_19767156) virus belonging to the 2.3.4.4b clade was selected for the ferret challenge. The challenge virus was isolated by inoculation of specific-pathogen free (SPF) (Charles Rivers Laboratories) 9-to-11-day-old embryonated chicken eggs. Eggs were incubated for 72 h at 37°C and candled daily. Dead embryos were chilled overnight at 4°C and allantoic fluids were harvested and tested by the hemagglutination (HA) test. Positive fluids were tested for the presence of bacterial contamination and stored at −80°C.

The following A(H5) HPAI viruses were used as HI antigens to test the breadth of reactivity of sera collected from vaccinated ferrets: i) A/Vietnam/1194/2004 (clade 1; EPI_ISL_30632), ii) A/turkey/Turkey/2005 (clade 2.2.1), iii) IBCDC-RG6 A/Anhui/1/2005 (clade 2.3.4; EPI_ISL_24603), iv) IDCDC-RG43A A/gyrfalcon/Washington/41088–6/2014 (clade 2.3.4.4c; EPI_ISL_173878), v) IDCDC-RG71A A/Astrakhan/3212/2020 (clade 2.3.4.4b; EPI_ISL_13655139), vi) IDCDC-RG63A A/duck/Bangladesh/17D1012/2018 (clade 2.3.2.1a; EPI_ISL_331119), and vii) A/duck/Vietnam/NCVD-1584/2012 (clade 2.3.2.1e; NIBRG-301, NIBSC-17/142).

Virus titrations were performed on confluent monolayers of MDCK cells, seeded at 3.75×10^4 cells per well in 96-well plates (Corning, 3596). Briefly, after 24-h incubation, confluent cell monolayers were incubated for 1 h at 37°C, 5% CO_2 with 50 μL of serial dilutions of the virus stock in cell culture medium deprived of FBS. After the incubation, 100 μL of the same medium was added to the inoculum in each well. After 72 h, the medium was removed and cells were fixed in 4% paraformaldehyde (PFA, Thermo Scientific, J61899.AK), for 30 min at 4°C. Upon removal, cells were permeabilised by incubation with a 0.5% Triton X-100 (Sigma, T8787) PBS solution for 10 min. Immunostaining of infected cells was performed by incubation of a mouse anti-Influenza A monoclonal antibody mix (1:4000) (Merck Millipore, MAB8257 and MAB8258 1:1) for 1 h, followed by a 1-h incubation with peroxidase-labelled goat anti-mouse antibodies (1:1000) (Jackson ImmunoResearch, 115–035–003) and a 7 min incubation with the TrueBlue (SeraCare, 5510–0030) peroxidase substrate. Solution of 1% bovine serum albumin (BSA) (Sigma/Merck, A9647) and 0.05% Tween 20 (Sigma/Merck, P2287) in PBS was used for the preparation of working dilutions of immuno-reagents. After the removal of the monoclonal antibody mix, wells were washed 4 times with the 0.05% Tween 20 (Sigma, T8787) PBS solution (Thermo Scientific, 18912014). For the titration of virus in organ supernatants, the protocol adopted to titrate the viral stock was modified to reduce cell toxicity through removal of the inoculum after incubation and washing with PBS before the addition of 150 μL of culture medium. The median tissue culture infectious dose ($TCID_{50}$) was calculated based on the Reed-Muench method.[78]

Mouse immunogenicity studies

For DNA immunogenicity studies, six mice (one group per antigen) were immunised subcutaneously (SC) on the rear flank with 50 μg DNA encoding DVX antigens and controls (Table S2A). The HA antigens, DVX-H5-1, DVX-H5-2, H5 controls A/Sichuan/26221/2014 (H5), A/gyrfalcon/Washington/41088–6/2014 (H5), and A/Anhui/2021–00011/2020 (H5) were given as two doses, 28 days apart (Figure 2A). Mice immunised with NA antigens DVX-N1, DVX-N6, N1 control A/Brisbane/02/2018 (N1) and N6 control A/yellow-billed teal/Chile/8/2013 (N6) received four doses on days 0, 14, 28 and 42 (Figure 2B). The DVX-M2 antigen and M2 controls A/Brisbane/2/2018 (M2) and A/Kansas/14/2017 (M2) followed the same immunisation schedule as the NA antigens (Figure 2B). The naive control group was administered 50 μL DPBS (−/−) (Thermo Scientific, 10010031).

For mRNA immunogenicity studies, six mice per vaccine antigen were immunised intramuscularly with 10 μg DVX-panH5Nx on D0 and D21. WIV control mice were immunised at D0 with 1.5 μg (Table S2B). Terminal blood samples were collected on D63. In a subsequent study, five mice per group were immunised with 5 μg DVX-panH5Nx_FML_2 and 1.5 μg $WIV_{2.3.4.4b}$ on D0 and D98 and terminal bleeds were collected on D224 (Figure S4C). Serum was processed by heat-inactivation at 56°C to deactivate complement, and stored at −20°C for serology.

Please cite this article in press as: Del Rosario et al., Broad vaccine protection against globally diverse influenza A/H5Nx viruses, Cell Reports Medicine (2026), https://doi.org/10.1016/j.xcrm.2026.103131

Mouse challenge studies

At 7 weeks of age, 132 mice (66 males and 66 females) were divided into sets of three (one for each challenge virus). Each set was vaccinated with different vaccine formulations (12 mice; 6 males and 6 females per vaccination group) (Table S2C), on days 0 and 21, and immunised with two intramuscular injections of vaccine (10 μg DVX-panH5Nx, 150 ng WIV) each given in 50 μL PBS to the quadriceps muscle of each hindlimb. Prior to virus challenge, mice were transferred to the BSL4 containment laboratory (NML) and housed in groups of 3 animals per HEPA-filtered cage. On day 49, each set was challenged with three HPAI H5N1 viruses (Table S2C) Mice were anesthetised using isoflurane delivered in 5% O_2 and 10LD_{50} (50% lethal dose) of virus in 50 μL neat MEM (Sigma, M0275) delivered by intranasal instillation. Four days post-challenge, 6 mice from each set (3 males and 3 females) were sacrificed to determine the influenza viral load in the lungs and spleens. The remaining 6 mice (3 males and 3 females) from each set were monitored for weight and clinical evaluations daily for 14 days or until an animal reached the mandated clinical endpoint. Clinical signs including weight loss, respiratory distress, ruffled fur, and hunched posture were scored. The humane endpoint was based on cumulative clinical score or weight loss above 25% of initial body weight or any signs of CNS infection including ataxia, paralysis, or loss of righting reflex. All mice that have lost ≥25% of their initial body weight were culled. On day 63 (14 dpc), all surviving mice were culled.

Viral titers in tissues were determined by $TCID_{50}$ assay. Frozen samples (−80°C) were thawed, weighed, placed in neat MEM (Sigma, M0275), and homogenised with a 5 mm stainless steel bead in a Bead Ruptor Elite Tissue Homogenizer (Omni) for 30 s at 4 m/s. Homogenates were clarified by centrifugation at 1500*xg* for 10 min and 10-fold serial dilutions in MEM/0.1% BSA (Sigma, A1470) were added in triplicate to washed confluent MDCK cells in 96-well plates with MEM (Sigma, M0275) containing 0.1% BSA (Sigma, A1470) and 0.5 μg/mL TPCK-trypsin (Sigma, T1426). Cytopathic effect was read three days post-infection and $TCID_{50}$ per gram of tissue was calculated by the method of Reed and Muench.[78]

Ferret challenge study

Animals were quarantined for 2 weeks and enrolled in the study upon testing negative for the presence of type A influenza antibodies. At 19 weeks of age, 18 ferrets were vaccinated with three different formulations (Table S2D). DVX-panH5Nx_FML2 ferrets ($n = 8$) were immunised a month later but underwent the same study schedule as the first three groups. Immunisation dose for DVX-panH5Nx was 100 μg, and 25 μg for DVX-panH5Nx_FML2 respectively. $WIV_{2.3.4.4b}$ ferrets were dosed with 3.8 μg WIV adjuvanted 1:1 with MF59 (InvivoGen, vac-adx-10), as adapted from literature.[79–81] All ferrets were immunised twice, on day 0 and on day 21, receiving a total of 0.8 mL of formulation via three intramuscular (IM) injections at distinct sites at the level of the hind legs. Blood samples were collected from each ferret on days 0, 21, 42, 50, and 63. On day 47, the animals were transferred into BSL3 animal facilities to allow for acclimatisation before the challenge. Each HEPA-filtered isolator (Montair, HM 1900) housed 2 animals. On day 49, ferrets were challenged through inoculation via the intranasal (IN) route with 200 μL of allantoic fluid containing 10^5 $TCID_{50}$ of the challenge virus. The challenge required that ferrets were maintained under surgical anesthesia induced by an intramuscular injection of a solution comprising Nimatek (100 mg/mL ketamine hydrochloride) and Domitor (1 mg/mL medetomidine hydrochloride) at a ratio of 1:1 (v/v), with an injection volume equal to 80 μL/kg of body mass. Anesthesia was reverted by an intramuscular injection of Antisedan (5 mg/mL atipamezole hydrochloride) to antagonise the action of the α-2 agonist Domitor.

Nasal washes were collected under surgical anesthesia from each group of ferrets on days 2, 3, 4, 6, 8, 10, and 12 post-challenge and were immediately stored at −80°C. Briefly, 1 mL of PBS was inoculated in each nostril and about 1.5 mL of nasal wash was collected in total for each animal in a 50 mL conical tube. Necropsy was conducted on both deceased and sacrificed ferrets at the end of the study. Ferrets were examined at the macroscopic level for the presence of lesions and a bronchoalveolar lavage (BAL) was carried out. Briefly, a catheter was placed in the trachea and 10 mL of PBS was injected in the lungs and about 5 mL of fluid was recovered and stored at −80°C. Moreover, the following organs were collected: cranial lung lobe, medial lung lobe, spleen, liver, brain, and pancreas. All organs were sampled and fixed in 10% neutral buffered formalin to perform histopathological and immunohistochemical analyses. Specimens from all organs, and a part from the brain, were stored at −80°C for virological analyses. On day 63, two weeks after the challenge, all surviving ferrets were sacrificed under surgical anesthesia by terminal exsanguination via cardiac puncture.

Temperature, body weight, and presence of clinical signs were monitored daily beginning three days before the challenge and for 14 days after the challenge. The temperature was recorded daily with the SureSense scanner (MSD Animal Health, HRPG1N) before the collection of samples. Clinical evaluation was carried out daily, at the same hour and was standardised through the adoption of a scoring system grading signs of disease as follows: 0 – alert and reactive subject irrespective of external stimulation, absence of respiratory signs; 1 – mild depression of the sensorium, reduced exploratory activity, engagement with the other ferret mate and reduction in the activity levels in response to external stimulation; nasal discharge or occasional sneezing; 2 – moderate depression of the sensorium, lethargy, exploratory activity and engagement with the other ferret mate are strongly reduced and are triggered only in response to external stimulation; frequent sneezing and/or labored breathing; 3 – alterations of the sensorium, state of stupor, hyperexcitability, marked depression, tremors and/or reduced tone of the hind legs, abnormal interaction in response to external stimulation (e.g., stereotypic movements, aggressivity in tame subjects), and dyspnoea; 4 – severe depression, severe neurological signs (e.g., ataxia, torticollis), inability to walk or feed; severe dyspnoea and diaphragmatic breathing. The humane endpoint was reached when animals were either assigned a score of 4, or in case of weight loss ≥20% of initial body weight (day 0).

CellPress OPEN ACCESS

Cell Reports Medicine
Article

Viral RNA quantification

Nasal washes and BAL were centrifuged for 2 min at 2000*xg*. Tissue samples were weighed and homogenised on a TissueLyser II (Qiagen) in a 1:10 (w/v) ratio with PBS supplemented with 1% of a 2:3 penicillin-streptomycin solution (10,000 Unit/mL) (Euroclone-ECB3001D) and a 1:3 nystatin solution (Sigma-Aldrich, N1638) (10,000 Unit/mL). Homogenates were centrifuged at 10,000*xg* for 1 min. Automated nucleic acid purification from all samples was performed using the MagMax CORE Nucleic Acid Purification Kit (Thermo Scientific, A32700) on a KingFisher Flex (ThermoFisher Scientific) according to manufacturer recommendations (workflow 'Simple'). Samples were subjected to viral genome quantification by digital RT-PCR (dRT-PCR) employing an oligonucleotide set targeting type A Influenza Viruses.[82] The PCR reaction mix consisting of the QIAcuity OneStep Advanced Probe Kit (Qiagen, 250131), 0.6 nM primers, 0.4 nM probe and 4 μL template was assembled with a Myra Liquid Handling System (Bio Molecular Systems, MYRA-LHS50). Amplification on a QIAcuity Digital PCR System (Qiagen, 911035) consisted of a reverse transcription step at 50°C for 40 min, reverse transcriptase (RT) inactivation at 95°C for 2 min, and 45 cycles of denaturation at 95°C for 5 s and annealing/extension at 62°C for 1 min. Data were analyzed with the QIAcuity Software Suite v. 2.5.0.1, with automatic threshold setting. Quantification data were converted to genome copies per 1 mL nasal/bronchoalveolar wash (GC/mL).

Histopathology

Following fixation, tissues underwent standard paraffin embedding and processing before hematoxylin and eosin (H&E) staining. Tissue pathology, e.g., for lungs - lesions, interstitial pneumonia, mononuclear phagocytosis, intrabronchial and intrabronchiolar inflammation, bronchial and bronchiolar epithelial cell necrosis, perivascular oedema, alveolar oedema, and neutrophil margination; and for brain – lymphocytic infiltration in the neuroparenchyma, encephalitis, gliosis, neuronophagia, and necrosis, was scored in blinded fashion in grades of 0 (absent), 1 (mild), 2 (moderate), to 3 (marked) (Table S5).

Serological investigations

Pseudotype neutralisation assay (pMN)

Serum neutralising titers post-immunisation against an H5 pseudotype virus panel (Table S3A) were determined via pMN.[50,83] Briefly, in a Nunc 96-well plate (Thermo Scientific, 136101), starting at a 1:100 dilution, serum samples were serially diluted 2-fold or 3-fold in complete DMEM across the plate. Control wells consisting of "pseudovirus only" (equivalent to no neutralisation) and "cells only" (equivalent to 100% neutralisation) were included. H5 pseudotype virus (1.0×10^6 RLU/mL (Relative luminescence unit)) was added to all wells except "cells only" wells and plates were incubated for 1 h at 37°C, 5% CO_2. After incubation, 1.5×10^4 HEK293T/17 cells were added to all wells and plates were incubated for 48 h at 37°C, 5% CO_2. Supernatant was discarded and 1:1 diluted Bright-Glo luciferase assay substrate (Promega, E2620) in PBS (Thermo Scientific,10010023) was added per well for 5 min. The plates were read using GloMax Navigator (Promega) using the Promega GloMax Luminescence Quick-Read protocol and values were calculated as relative luminescence units/mL (RLU/mL).

Pseudotype enzyme linked lectin assay (pELLA)

Neuraminidase inhibition titers against an N1, and N6 pseudotype virus panel (Table S3B) were determined via pELLA.[53,83] Briefly, Nunc clear Maxisorp plates (Thermo Scientific, 439454) were coated with 25 μg/mL Fetuin (Sigma, F3385) and incubated at 4°C. Next day, 1:100 dilution of serum samples were serially diluted 2-fold in sample diluent (SD) (1% (w/v) Bovine Serum Albumin (BSA) (Sigma, A2153) and 0.5% (v/v) Tween 20 (Sigma, P1739) in PBS (Thermo Scientific, 14040091) across the plate. Fetuin coated plates were washed three times with Wash buffer (WB) (0.5% (v/v) Tween 20 in PBS) and serum dilutions were transferred to fetuin plates. Control wells with "pseudotype virus" only (equivalent to no NA inhibition) and SD only (equivalent to 100% NA inhibition) were also included. NA pseudotype virus was added to all wells except the SD control wells and plates were incubated overnight at 37°C, 5% CO_2. Next day, plates were washed six times and conjugate solution (1% (w/v) BSA, 1 μg/mL of lectin from *Arachis hypogaea* (peanut) peroxidase conjugate (Sigma L7759) in PBS (Thermo Scientific, 14040091)) was added. Plates were incubated while shaking (350 rpm) for 2 h. After incubation, Plates were washed and 50 μL per well of 1-Step Ultra TMB-ELISA Substrate Solution (Thermo Scientific, 34029) was added. The plates were incubated for 10 min and reaction was stopped by adding 50 μL 0.5 M HCl (Acros Organics, 124630025). The plates were read at optical density (O.D.) 450 nm using Microplate reader (Agilent, BioTek 800 TS). The IC_{50} was determined as the inverse of serum dilution that resulted in 50% inhibition of NA activity using GraphPad Prism 10.4.1.

Hemagglutination inhibition assay (HI)

One volume of serum was mixed with four volumes of receptor-destroying enzyme (RDE) Seiken (Deben DiagnosticsLtd, 370013) and incubated for 12–18 h at 37°C, followed by an inactivation step at 56°C for 30 min. The HI tests were conducted in accordance with standard procedures.[84] In a 96-well V-bottom microtitre plate (Griener Bio-one, M8185), 1:10 RDE treated serum was serially diluted 2-fold in PBS (Gibco, 10010–015). Control wells containing PBS and RBCs only were also included. Four HAU of virus (Table S3D) was added to all wells except the control wells and the plates were incubated for 30 min at room temperature. After incubation, 0.5% chicken RBCs (TCS biosciences, FB013AP) was added to all wells and plates were incubated again for 1 h at room temperature. The HI titer was determined by the highest dilution of serum that resulted in complete inhibition of 4 HAU virus. For the purposes of statistical analysis and graphic representation, a value of 1:5 (2.32 Log_2) was assigned to negative samples.

ELISpot

To quantify IFN-γ-secreting T cells, we employed an ELISpot assay adhering to Mabtech's Ferret IFN-γ ELISpot Plus kit protocol (Mabtech 3112-4APW-2). Fresh peripheral blood mononuclear cells (PBMC) were isolated using vacutainer CPT tubes (BD

Please cite this article in press as: Del Rosario et al., Broad vaccine protection against globally diverse influenza A/H5Nx viruses, Cell Reports Medicine (2026), https://doi.org/10.1016/j.xcrm.2026.103131

Biosciences, 362753), washed with PBS (Thermo Scientific, 10010–015) and resuspended in complete RPMI 1640 medium (Thermo Scientific, 21875034) supplemented with 10% FBS (Thermo Scientific, A5256801), 1% penicillin-streptomycin (Thermo Scientific, 15140–122), and 1% L-glutamine (Thermo Scientific, 25030081). Pre-coated plates were conditioned with RPMI 1640 medium containing 10% serum for 30 min at room temperature. Cells were stimulated under three conditions: PMA/Ionomycin (1×10^5 cells/well), Whole Inactivated Virus (2×10^5 cells/well, 100 HAU/mL[85] of A/chicken/Italy/23VIR3799-1/2023 (H5N1)), and unstimulated controls (2×10^5 cells/well). Cells were plated in triplicate in complete RPMI and incubated for 24 h at 37°C, 5% CO_2. Following incubation, plates were washed with PBS and detection antibody (MTF19-biotin, 0.5 μg/mL) was added. After washing again, streptavidin-alkaline phosphatase (ALP, 1:1000) was added to each well. BCIP/NBT-plus substrate solution was added for spot development, and plates were incubated at room temperature in the dark until spots became visible. The reaction was stopped by rinsing the plates with water. Spot-forming units (SFU) were quantified using an automated ELISpot reader (CTL-Immunospot S6 Ultra Analyzer). The relative ELISpot response was calculated as the ratio of the mean SFU from whole inactivated virus-stimulated samples to the mean SFU from unstimulated samples.

Luminex assay to detect anti-M2 antibodies

Recombinant Influenza A H5N1 M2 protein (A/chicken/Hebei/326/2005 (H5N1) (Accession- ABC74394.1) (Stratech, LS-G56682-LSP) was coupled to Bio-Plex Pro magnetic COOH beads (Bio-Rad, MC1-0014-01) using Adipic acid dihydrazide (ADH) (Sigma, A0638). Negative control beads (Bio-Rad, MC1-0100-01) that were not coupled to any protein were also included. In a U-bottom microplate, 50 μL of sera was diluted in 1% (w/v) skimmed milk in PBS. The Nunc black plates (Greiner bio-one, 655077) were placed on a Bio-Plex Handheld Magnetic Washer (Bio-Rad, 171020100), 50 μL per well of 1.5×10^5 coupled beads were vortexed, pooled and plated. The liquid was discarded and sera were transferred to the beads on the plate. Control wells consisting of 1:100 blocking buffer (0.5 mg/mL blocking solution (Candor-bioscience,110125) and 0.05% (w/v) Sodium Azide (Sigma, S2002) diluted in skimmed milk (Millipore, 70166-500G), were included. The plates were incubated with shaking (500 rpm) at 37°C for 2 h. After incubation, plates were washed three times with Wash Buffer (WB) (0.05% (v/v) Tween 20 in PBS). Fifty microliters of anti-mouse (Abcam, ab97024) or anti-ferret (Novus Biologicals, NB7222PE) secondary antibody labeled with fluorescent phycoerythrin (PE) dye was added to the wells followed by incubation for 30 min. After incubation, plates were washed thrice with WB and read via the Bio-Plex 200 System (Bio-Rad, United States). The data is reported as Median Fluorescence Intensity (MFI) minus background, with background being a no serum control plotted using a non-linear sigmoidal 4-point plot, where x is log fold-dilution of serum and y is MFI.

Strain-specific IgG ELISA

Nunc clear Maxisorp plates (Thermo Scientific, 439454) were coated with 5 μg/mL Influenza Antigens (Table S3E) and incubated at 4°C. Next day, plates were washed thrice with WB (0.1% (v/v) Tween 20 in PBS (Thermo Scientific, 10010031), blocking buffer (0.2M (w/v) Tris-base (Fisher Scientific, 10103203), 1% (w/v) BSA (Sigma, A2153) in PBS (Thermo Scientific, 10010031)) was added to the plates and incubated on shaking (300 rpm) at 37°C for 2 h. Starting at 1:100 dilution, the ferret serum samples were serially diluted 5-fold in blocking buffer. These dilutions were transferred to the coated plates and incubated as mentioned previously. The plates were washed thrice and secondary antibody, horseradish peroxidase conjugated anti-ferret IgG (1:2000) (Abcam, AB112770) was added to all wells and incubated for 1 h. Plates were washed again and 1-Step Ultra TMB-ELISA substrate solution was added to the plates and timed for 3 min 0.5 M HCL (Fisher Scientific, 10499360) was added to stop the reaction. The plates were read at optical density 450 nm (OD_{450}) using Microplate reader (Agilent, Bio Tek 800 TS).

IgG competition ELISA and indirect ELISA

Serum samples were also assayed using two enzyme-linked immunosorbent assay (ELISA) kits, namely the ID Screen Influenza H5 Antibody Competition 3.0 Multi-Species (IDVet, FLUACH5V3 ver 0724 EN) and an in-house modified version of the ID Screen Influenza H5 Indirect (IDVet, FLUH5S ver 1221 EN). Both assays rely on the use of plates coated with an HA protein derived from a 2.3.4.4 clade virus.

This competition ELISA (FLUACH5V3 ELISA kit) is designed to detect the antibodies directed against the H5 hemagglutinin of the Influenza A virus in avian and mammalian samples. Plates were pre-coated with a recombinant H5 hemagglutinin. The protocol for chicken and turkey sera was adopted hence, requiring a 1:2 dilution of serum (v/v) in Dilution Buffer 14 and an incubation in the microplate for one hour at 37°C. If anti-H5 antibodies are present in the test samples, an antibody-antigen complex will form which masks the H5 epitopes. After washing the plates, an anti-H5 peroxidase (HRP) conjugate is added which binds to the remaining free H5 epitopes forming an antigen-conjugate-HRP complex. A substrate is then added which binds to the antigen-conjugate-HRP complex resulting in coloration which is measured at Optical Density (O.D.) 450 nm. The intensity of the signal measured is inversely proportional to the amount of H5 antibodies present in the test samples. The results were expressed as S/N ratio % (positive $S/N \leq 60$; doubtful $40<SN<60$; negative $S/N \geq 40$).

The ID Screen Influenza H5 Indirect (IDVet, FLUH5S ver 1221 EN) ELISA kit is designed to detect the antibodies directed against the H5 hemagglutinin of the Influenza A virus in the serum, plasma, or egg yolk samples from chicken, turkey, duck and goose. The kit was modified to react with the ferret species and to ensure that the performance of the kit was in a linear range. The plates were pre-coated with a recombinant H5 hemagglutinin. If anti-H5 antibodies are present in the test samples, it will form an antibody-antigen complex. Briefly, sera were diluted 1:3200 (v/v) in Dilution Buffer 14 and incubated in the microplate for one hour at 37°C. After removal of the samples and multiple washes, wells were incubated with an anti-dog HRP-conjugated antibody (available on request from IDvet) diluted 1:10 (v/v) in Dilution Buffer 1 (available on request from IDvet). For control wells, the kit HRP-conjugated antibody was used at a 1:10 dilution in Dilution Buffer 3 according to the instruction manual. The detection step was carried out by incubation of

wells with 100 μL of the kit Substrate Solution followed by addition of 50 μL of the kit Stop Solution. The cut-off value was calculated using the standard formula "cut-off = mean Optical Density (O.D.) of negative controls +3 × standard deviation" and was set at an O.D. of 0.089. Archive sera collected from naive ferrets were used as negative controls. The intensity of the signal measured is directly proportional to the amount of H5 antibodies present in the test sample.

All ELISA assays were read with a Sunrise (Tecan) absorbance microplate reader and O.D. were recorded at 450 nm.

QUANTIFICATION AND STATISTICAL ANALYSIS

The statistical details of experiments can be found in the figure legends and supplemental document. All statistical analyses were performed with RStudio. Statistical tests used include Wilcoxon rank-sum test (rank-based nonparametric test), Kruskal-Wallis followed by post-hoc Dunn's test (two-step non-parametric test) and unpaired t-tests where 'n' represents the number of animals per immunisation group. The Benjamini-Hochberg Procedure was applied to reduce the probability of false positives in the comparison of multiple groups. For all models, only significant p values ($p < 0.05$) are indicated on the figures and all other p values are listed in supplementary tables.